University of Alberta

Library Release Form

Name of Author: David V. Hildebrand

Title of Thesis: The Utility of Medium Wavelength Imaging Radar from JERS-1 for Operational Soil Moisture Monitoring in Central Alberta, Canada

Degree: Master of Science

Year this Degree Granted: 2003

UNIVERSITY OF ALBERTA

The Utility of Medium Wavelength Imaging Radar from JERS-1 for Operational Soil Moisture Monitoring in Central Alberta, Canada

By

David V. Hildebrand

Ⓒ

A thesis submitted to the Faculty of Graduate Studies and Research in partial fulfillment of the requirements for the degree of Master of Science

In

Water and Land Resources

Department of Renewable Resources

Edmonton, Alberta

Fall, 2003

University of Alberta

Faculty of Graduate Studies and Research

The undersigned certify that they have read, and recommended to the Faculty of Graduate Studies and Research for acceptance, a thesis entitled "The Utility of Medium Wavelength Imaging Radar from JERS-1 for Operational Soil Moisture Monitoring in Central Alberta, Canada" submitted by David V. Hildebrand in partial fulfillment of the requirements for the degree of Master of Science in Water and Land Resources.

Acknowledgments

Abstract

Experimental observations indicate that radar imagery may be used to detect soil water at depth because microwaves in the longer wavelengths tend to penetrate better than those at short wavelengths. However, experimental observations may not always be applicable to field conditions because physical landscape factors may also affect penetration. In this study the utility of medium-wavelength radar imagery for detecting soil moisture in the field in an actual soil moisture monitoring program was tested. Soil moisture data were collected in the field as part of an operational sampling program and then compared with JERS-1 image data. Ancillary data to determine the influence of other factors on backscatter were collected from a variety of sources including LANDSAT Thematic Mapper imagery, soil surveys and digital elevation models. The JERS-1 image data could not be used to reproduce soil moisture data in an operational monitoring program, perhaps due a number of factors including low soil moisture variability, inadequate field sampling precision (specifically timing) and/or lack of surface cover information. This finding does not negate the use of radar imagery for soil moisture mapping. However, it calls into question its utility in operational soil moisture monitoring under current circumstances.

Contents

Figures

Tables

Chapter 1   <u>Introduction</u>

1.1 *Purpose and Study Area*

The recent interest in global climate modeling has resulted in expanded efforts to more accurately model soil moisture for the purpose of land surface parameterization in models. The Global Soil Wetness Project (Dirmeyer *et al.*, 1999) illustrates the world-wide interest in global soil moisture modeling. Each spring and fall Alberta Agriculture, Food and Rural Development (AAFRD) conducts a survey of soil moisture conditions (Howard, 2000). These data are then used to map general soil moisture conditions.

Remote sensing has increasingly played a role in that modeling process (Ferraro *et al.*, 1996; Running, 1991) because of its ability to collect data over wide areas at frequent intervals. Radar imaging, in particular, has shown promise due to its penetration capabilities and the unique response of microwaves to water molecules in surface materials.

The principle objectives of this study were to determine the extent to which moisture in the soil can be detected by medium-wavelength Synthetic Aperture Radar[1] (SAR) from the JERS-1 (JERS) satellite and to study the extent to which other factors influence backscatter. The study utilizes a subset of the AAFRD soil moisture survey data for calibration.

The study area was selected by consulting the JERS footprints and maximizing the number of field sample points within an image (minimum = 4) while minimizing the

---

[1] RADAR is the common acronym for <u>Ra</u>dio <u>D</u>etection <u>an</u>d <u>R</u>anging. It is used here in the form of common usage (i.e., with lower and mixed case).

cloud cover of the corresponding LANDSAT-TM (LANDSAT) image. The images closest to the field sampling dates were then acquired for the study. Since the exact field sampling dates were unknown mid-April and mid-October were assumed. Two candidate areas emerged from this process, one in Central Alberta (spring 1995) and one in Northern Alberta (spring of 1993). Due to the cost of image data only the Central Alberta area was chosen. The study area as shown in Figure 1.1.
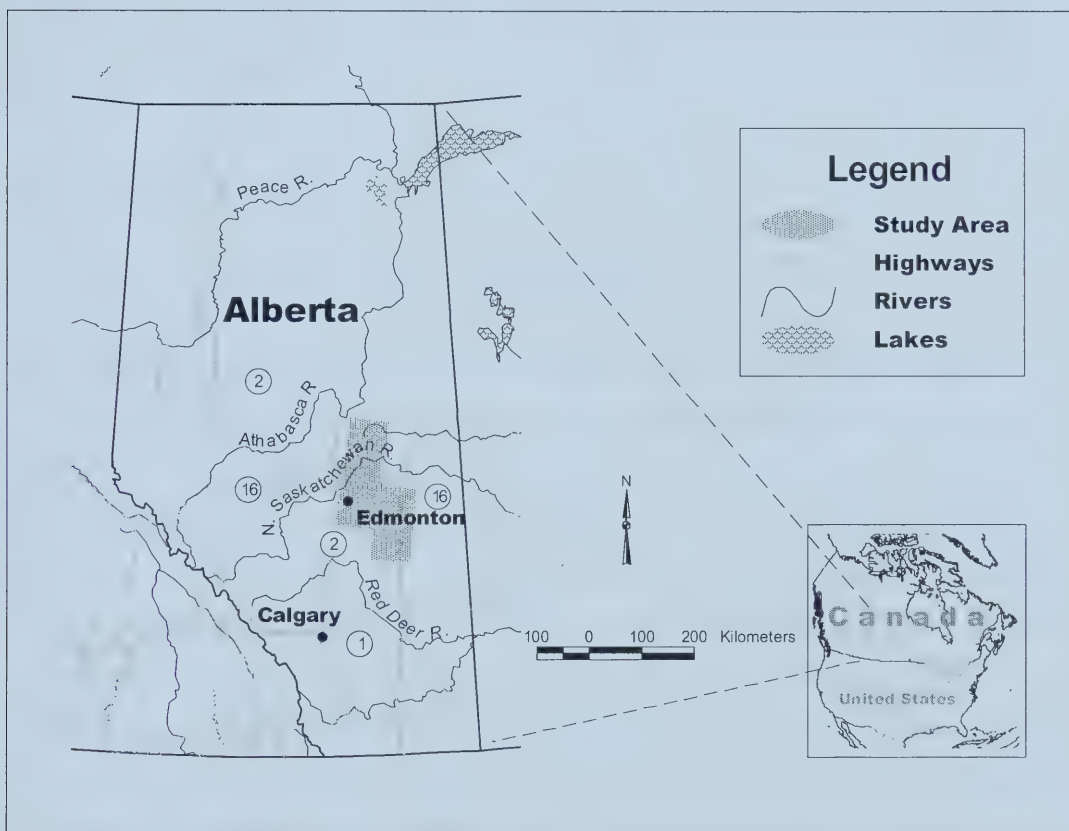
Figure 1.1   Location of study area

Ecologically, the study area is located primarily in the Central Parkland Subregion of the Parkland Region in the south and the Dry Mixedwood Subregion of the Boreal Forest Region in the north (Strong and Thompson, 1995). Approximately 80% of the land in the study area has been cleared for agriculture.

The Central Parkland Subregion terrain is characterized by undulating morainal material

with slopes less than or equal to 5°. The dominant soils are Black Chernozems with well to moderately drained. Natural vegetation is primarily herbaceous.

The Dry Mixedwood Subregion is characterized by a more varied terrain than the Central Parland Region, and consist of rolling to undulating moraine and level to undulating lacustrine plain interspersed with organic terrain. Slopes are less than or equal to 9°. The dominant soils are Gray Luvisols and Organics with generally moderate drainage. Natural vegetation is closed deciduous and mixedwood forest with a significant shrub component.

1.2 Background

1.2.1 General Imaging Radar Considerations

The operational principles of imaging radar are centred around microwave energy transmitted in pulses from an active source and then being echoed back from the target. Figure 1.2 illustrates these principles. Radar echoes are recorded as signal strength and then converted to image tone. The fact that the energy source "illuminates" the target in an off-nadir configuration, and that echoes take longer to reach the antenna from the far range compared to the near range, gives the image two-dimensional properties. If a target reflects all or most of the signal back to the antenna the image will appear light. Conversely, if a target reflects most or all of the signal away from the antenna, or absorbs the signal, the image will appear dark. Various targets behave differently depending on their geometry relative to the incidence angle of the antenna, and their reflective properties, and this creates the variable image tone and texture.
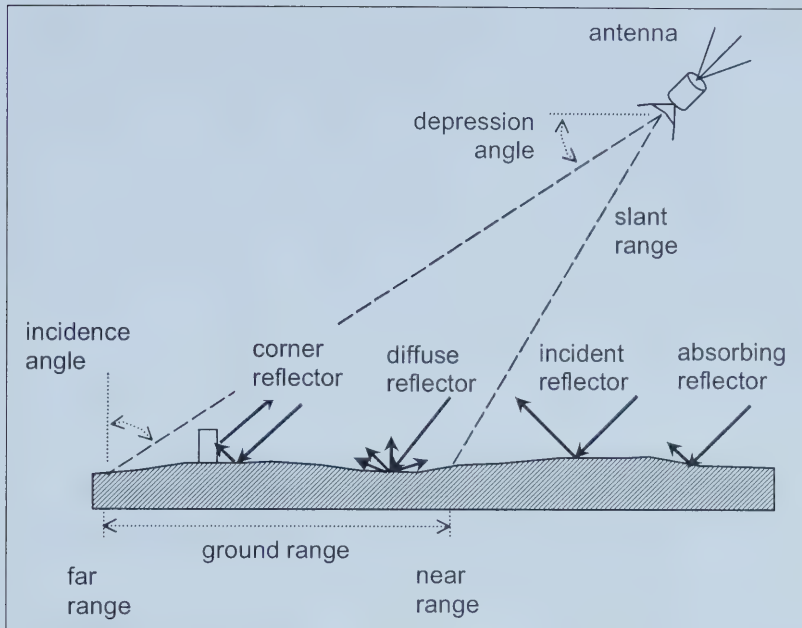
Figure 1.2   Imaging radar characteristics

Spatial resolution is constrained by the aperture of the system, which is a function of antenna length. Synthetic Aperture Radar (SAR) imaging systems synthesize a larger aperture by generating multiple "looks" on a target and characterizing Doppler shift in order to generate a higher resolution image (Lillisand and Kiefer, 2000). However, this causes the resulting image to appear speckled.

Radar imaging systems operate in the microwave frequencies as shown in Table 1.1. In addition, imaging systems may include switching mechanisms allowing them to receive energy in either the same or opposite polarization to which it was transmitted. Thus, four combinations of horizontal and vertical polarizations, HH, VV, HV and VH, are possible. The first letter represents the polarization of the transmitted pulse and the second that of the received energy.

Table 1.1   Radar imaging wavelengths and frequencies (Lillisand and Kiefer, 2000)

Band	Wavelength (cm)	Frequency (GHz)
K_a	0.75 – 1.1	40 – 27.3
K	1.1 – 1.67	27.3 – 18.0
K_u	1.67 – 2.4	18.0 – 12.5
X	2.4 – 3.75	12.5 – 8
C	3.75 – 7.5	8 – 4
S	7.5 – 15	4 – 2
L	15 – 30	2 – 1
P	30 – 100	1 – 0.3

1.2.2   Considerations for Imaging Soils by Radar

The penetration of soil by microwaves is critical to the notion of soil moisture detection. Microwave penetration requires smooth, fine-grained, homogeneous material. The larger the size of material the greater the scattering (Roth and Elachi, 1975). Elachi *et al.* (1984) also noted that low incidence angles are required for good penetration. Wavelength reduction occurs at the surface due to refraction and this may have an effect on subsurface backscatter.

There is empirical evidence for radar penetration of surface material and the potential that exists for detection of soil moisture. However, it is important to note the other factors which can have an effect on radar penetration and, hence, backscatter. The most important factors are surface roughness, the complex dielectric constant and vegetative cover (Holmes, 1990). These factors are examined below.

Surface Roughness

Surface roughness probably has the greatest effect on radar returns. The height of the land surface irregularity relative to the wavelength and incidence angle determines the reflective behavior of the surface. Major *et al.* (1993) noted that for C-HH radar at high incidence angles the backscatter was a function of surface roughness. The same results were confirmed for K_u-HH radar by Smith and Major (1996). Xu *et al.* (1998), in

5

studying the spectral (including microwave) properties of organic soils with RADARSAT data at incidence angles from 53 to 80 degrees, concluded that radar returns were more dependent on surface roughness and field management than on soil moisture. McCairn *et al.* (1996), in an experiment with ground-based scatterometer measurements using L-, C- and K_u-bands in all polarization modes, with 5 different incidence angles, noted that backscatter was significantly correlated with surface roughness at high incidence angles. Different combinations of wavelength and polarization all yielded similar results. Geng *et al.* (1996) reported that VV polarization was more sensitive to surface roughness than HH polarization but concluded that within-field variability of surface roughness contributed negligibly to within-field backscatter variability due to within-field uniformity of management practices.

Boisvert *et al.* (1996b) concluded that backscatter related to surface roughness tends to mask out backscatter related to soil moisture at larger incidence angles but that the effect of incidence angle on backscatter decreases as surface roughness increases. Ulaby *et al.* (1978) suggested that the optimum incidence angle for soil moisture detection is between 10 and 20 degrees.

In summary, while surface roughness is an important environmental parameter controlling backscatter, the way in which it is characterized depends on the nature of the research being done. Certainly if a regional picture is being constructed which takes into account various types of environments and field management practices, then it is necessary to account for surface roughness by using appropriate polarization as well as small incidence angles. However, for field-level studies where there is assumed to be little variation it may be appropriate to assume surface roughness to be constant.

Complex Dielectric Constant

For a given radar configuration, microwave penetration depth varies with the complex dielectric constant of the material being imaged. The complex dielectric constant is related to the strength of molecular bonding in a particular substance and, hence, its

resistance to molecular alignment (polarization) in the presence of an electrical field. Substances with a low complex dielectric constant have a greater electrical capacity and can hold a charge better than substances with a high complex dielectric constant. Water has an exceptionally low electrical capacity and, hence, has a high complex dielectric constant. This property also makes it resistant to microwave penetration.

Soil moisture can be related to the complex dielectric constant by a polynomial relationship (Topp *et al.*, 1994; Hallikainen *et al.*, 1985; Dobson *et al.*, 1985). Values of the complex dielectric constant range from 3 to 16 for most dry rocks and soils, and up to 80 for water with impurities. Moist soils have values typically between 30 and 60. Factors impacting the dielectric constant of soil are those which affect water holding capacity (texture, bulk density and organic matter) as well as salinity and temperature. Microwave penetration depth varies with the dielectric constant (Boisvert *et al.*, 1995b) as was demonstrated by Robinson *et al.* (1999). Generally, for dry soils in Canada the penetration is in the order of the SAR wavelength (Boisvert *et al.*, 1995a). Research has also shown, however, that it is possible to detect subsurface conditions up to 1 meter in dry desert sands with C-band data from RADARSAT (Robinson *et al.*, 1999). Normally, the penetration of C-band microwaves is in the order of approximately 50 mm but that under certain conditions (e.g. extremely dry) depth of penetration may, in fact, be independent of wavelength.

Smith and Major (1996) suggest that at the L-band wavelength soil moisture is the primary determinant of backscatter. Certainly L-band radar has the greatest capacity for penetration due to its long wavelength. Furthermore, it has been found that for C-band radar the highest correlation between backscatter and soil moisture is only between 0 and 2.5 cm depth. (McCairn *et al.*, 1996). It was also found, in the same study, that soil moisture was significantly correlated with backscatter at low incidence angles. This implies that surface penetration, enabled by long wavelengths and low incidence angles, is essential for detecting soil moisture.

Crop Residue and Vegetation Cover

Smith and Major (1996), in an experiment on backscatter and crop residues, noted that after irrigation the crop residue had a significant impact on backscatter in K_u and C-HH configurations. However, crop residue had no significant impact on backscatter in the L-HH configuration. Cross-polarization was better suited for identifying dry crop residues than like-polarization. Under moist conditions the separation of residue covered and bare fields was possible using a ratio of K_u and C-bands with a dual incidence angle (10 and 50 degrees) or a comparison before and after a rainfall or dew event.

Free water in the canopy, such as after a rainfall or dew event can enhance the separability of residue covered and bare soil fields (Brisco *et al.*, 1989; Gillespie *et al.*, 1990). Boisvert *et al.* (1996b) concluded that the vegetation cover structure coupled with plant moisture content and free water (dew and rainfall) as well as phenological stage affect radar returns. They also concluded that small incidence angles help to "see through" the vegetation cover.

Crevier *et al.* (1995) used time series ERS-1 SAR imagery to evaluate backscatter of various land covers with seasonal changes. They noted that bare fields exhibited the greatest change in backscatter followed by pasture. This indicates that moisture changes in the soil were the most evident in these types of land cover because the nature of the surface was relatively constant over time.

1.2.3 Application of Radar Imagery for Characterizing Soil Moisture

The application of radar imagery to soil moisture studies involves not only the soil moisture estimation itself but also taking account of other factors which may confound the estimation.

Soil Moisture Estimation

It is possible to estimate actual soil moisture through models once an image signature has been established. In a major experiment in Oxford County, Ontario the investigators found significant relationships between soil moisture and radar returns (Brown *et al.*, 1991; Brisco and Brown, 1992). Geng *et al.* (1996) observed a high correlation between soil moisture and backscatter using a C-HH configuration and were able to construct a linear model and derive a map of surface soil moisture. Biftu and Gan (1999) found a high correlation between C-band RADARSAT imagery and soil moisture in a variety of surface cover condition, both by using linear regression as well as by physical soil moisture modeling. The problem with using regression techniques to relate backscatter to measured soil moisture is that soil moisture measurements represent an area of about 5 cm^2 while a pixel integrates the values for an area represented by the spatial resolution of the sensor which is often an area of many square meters. Therefore, the method is extremely sensitive to the ground truth data used for calibration.

The scale of modeling is important when designing a ground truth sampling strategy, especially when considering the sensitivity of model calibration. Rotunno *et al.* (1996), found very low correlation within fields when trying to model backscatter and soil moisture using ERS-1 SAR data. However, when interpolation was done for the entire basin the correlation was much higher. Field-level descriptive statistics had been collected in that study and semivariograms used to characterize spatial variability. As a result, a geostatistical approach was recommended for interpolating soil moisture estimates for entire basins. Pietroniro *et al.* (1992) found that soil moisture correlated fairly well with backscatter when ground truth observations were aggregated for entire fields. They found that the observed relationship could be extended throughout the basin to sites of similar cover type and slope.

Surface Characteristics

Surface roughness must be considered when using imaging radar. Change detection can be used to eliminate effects of surface roughness as long as the detection period is short

enough that surface roughness remains constant and the only change is in soil moisture (Dobson and Ulaby, 1986; Brown *et al.*, 1993). In addition, with change detection a drying trend over the change period can be better detected than the spatial variability of soil moisture at a single point in time (Ladson and Moore, 1992).

Vegetative cover and crop residue are probably the most important surface characteristic which must be considered. The characterization of surface cover must be determined independently of radar imaging so as not to bias the results. Given the wide range and variable nature of vegetative cover, Owe *et al.* (1988) suggested that it would be possible to minimize the impact on radar returns by using satellite-derived vegetation indicies to improve the estimation of soil moisture, at least at the basin level.

The use of imagery for characterization of crop residue has a long history. Gausman *et al.* (1975) reported being able to discriminate bare soil from crop residue using visible and near-infrared wavelengths. A variety of brightness indicies based on a ratio of these wavelengths have been proposed in order to characterize crop residue (Major *et al.*, 1990; McNairn and Protz, 1993; Smith *et al.*, 1995). McNairn and Protz (1993) used ancillary soil texture data and found an improvement in the performance of their index. Leblon *et al.* (1996) and Smith *et al.* (2000) found that, in general, such indicies performed relatively well, especially with dry residue. However, they also noted a degree of inconsistency primarily due to soil background and tillage practice.

Crop residues, because of their ability to absorb water and also dry out quickly, will often exhibit a change in reflectance characteristics with environmental conditions, particularly moisture. Su *et al.* (1995) were able to separate oat residue from background soil using principle components analysis. Using PCA they were able to distill the variance in reflectance and then estimate residue from the component loadings and achieve good results. McMurtrey *et al.* (1993) found that, although differentiation between residue types in various soil conditions was not completely unambiguous, the major differences were captured at 450 nm, 660 nm and 830 nm and, therefore, Thematic Mapper (TM) bands detecting reflectance in those wavelengths could be used effectively. Daughtry

(2001) showed rather conclusively that residue water content had a significant impact on discrimination between soil and residue. Given that soil colour is impacted by moisture that conclusion is not surprising.

The above studies of crop residue reflectance occurred primarily as controlled field experiments. To deal with inconsistencies in an operational situation, Zhuang *et al.* (1991) used digital ownership boundaries and enforced the uniform classification of whole fields through a neural network classifier. They found that accuracy increased dramatically because site-specific anomalous situations could often be ignored. Their findings illustrate the importance of context when classifying an image, particularly when spectral classes may overlap to a certain extent.

1.3 Experimental Approach

The hypothesis in this study is that backscatter from L-band imagery is related to soil moisture as determined by the AAFRD soil moisture survey. L-band radar is employed because of its potentially better penetration capabilities than C-band radar. The approach taken in this study is to model backscatter, characterized as uncalibrated grey-level values from JERS imagery, in terms of factors discussed above which can be characterized at the same spatial resolution as JERS imagery. Factors which can only be characterized by field sample site, or training site, such as soil moisture, are then examined to determine the extent to which they may contribute to backscatter.

Using this approach it is assumed that the soil moisture conditions described at each site are representative for the site and that changes in soil moisture between the imaging date and the soil moisture survey date is not significant. The relationship of soil moisture to environmental factors was not considered on its own. The argument for including these measurements in the study could easily be made from a theoretical perspective but the scope of the study was not to examine soil moisture characteristics and behavior but rather, to establish the extent to which JERS imagery could be used for detecting and spatially discriminating soil moisture at various depths in relation to the current AAFRD soil moisture mapping program.

Chapter 2   Materials and Methods

A variety of software was employed in this study including ArcView GIS Version 3 (Environmental Systems Research Institute), EASI/PACE Version 6 (PCI Geomatics), S-Plus Version 6 (Insightful) and SAS Version 8 (SAS Institute)[2]. The capabilities of ArcView GIS and EASI/PACE were very similar in terms of the requirements of this study and their roles could have been easily interchanged. However, due to the flexibility of ArcView GIS and its customization capabilities much of the processing was done using ArcView GIS.

2.1 Data Considerations

2.1.1 Soil Survey Considerations

Soil Landscape Surveys

The Agricultural Region of Alberta Soil Inventory Database (AGRASID), housed at AAFRD, is a synthesis of soil surveys throughout the agricultural area of Alberta which have been digitized and brought into a common frame of reference (CAESA-Soil Inventory Working Group, 1998). Ecological land units and soil landscape models are delineated and described. The surveys have identified the landform model, described in MacMillan and Pettapiece (2000), for each unit and the soils, as well as their relative proportions, occurring in a particular unit. Some common chemical and physical properties, generally derived from pedo-transfer functions, are also given for each soil series found in a soil-landscape unit. The AGRASID data set is intended to be used at a scale of 1:100,000.

---

[2] Names are provided here for information purposes only. Their use does not constitute an endorsement of the products.

Soil surveys, including AGRASID, record repeating patterns which are observed between soils and landform position. However the tacit knowledge of the actual relationships acquired during the survey process is rarely captured because of the conceptualized nature of the soil-landscape model (Hudson, 1992). As a result of this deficiency MacMillan *et al.* (2000) developed an expert system to associate specific soils to landform position based on a particular soil's genetic pre-disposition. The system used an expert rule base which identified soil attributes that could be consistently related to landform position. Each soil was then rated as to the likelihood of occurring in a specific landform position. Using the information in AGRASID as well as quantitative morphometric landform information from MacMillan and Pettapiece (2000), each soil-landscape unit was characterized by the soil most likely to occur in one of the four landscape positions within that particular unit. This resulted in a some landscape units having more than one soil and some soils being included in more than one landscape position. The situation can be illustrated by the fictitious example in Table 2.1 where a soil-landscape unit has a well drained *ABC* soil occupying 60% of the unit and an imperfectly drained *DEF* soil occupying 40% of the unit. The slope configuration in the landform of the unit is defined as *Upper* – 20%, *Mid* – 50%, *Low* – 20% and *Depression* – 10%.

Table 2.1   Example of soil-landscape unit partitioning (MacMillan *et al.*, 2000)

Soil (ABC_6DEF_4)	Landform Position $(U_2M_5L_2D_1)$	Soil-landscape Partitioning (%)
ABC	Upper	20
ABC	Mid	40
DEF	Mid	10
DEF	Lower	20
DEF	Depression	10

Using this information it is possible, to a degree of accuracy commensurate with the accuracy of the original soil landscape survey, to characterize any given site in terms of the soil(s) most likely to be found at that particular site and, in turn, make inferences about site properties.

Soil Moisture Surveys

The field sampling sites for the soil moisture monitoring program conducted by AAFRD remain consistent from one year to the next and have been selected to represent the general landscape conditions of the surrounding area (Howard, 2000). In addition, the fields in which the sites are located are being continuously cropped, generally with wheat or canola. Several soil cores are taken with a King tube (approximately 4 cm diameter) on each site in order to get an adequate sample of the soil at that site. The representative cores are manually characterized, in terms of available soil moisture relative to field capacity and permanent wilting point, and the conditions recorded for the site. A site may be characterized, for example, by a soil which is wet from 0 to 10 cm, moist from 10 to 50 cm and dry from 50 to 100 cm. The nominal moisture classes which are used are defined in Table 2.2. Hand-texturing is also performed to determine texture class at the site and if the texture varies within the soil this is also noted.

Table 2.2 Available soil moisture class definitions used by AAFRD

Soil Moisture Class	Proportion of Available Soil Water Capacity
wet	1.00
moist/wet	0.75
moist	0.50
moist/dry	0.25
dry	0.00

Relationships between soil texture and moisture retention have been demonstrated and exploited by Oosterveld and Chang (1980) to develop equations for approximating gravimetric water content at field capacity (33 kPa) (FC) and at permanent wilting point (1500 kPa) (PWP). The equations were developed for a wide range of textures in Southern Alberta, conditions which are very similar to the study area in this investigation. The equations require sand and clay content in percent by weight as well as mean depth of sample in centimeters. Table 2.3 shows the median sand and clay content, taken from the textural triangle, for selected texture classes.

Table 2.3   **Particulate sand and clay content for selected texture classes from the textural triangle (Soil Classification Working Group, 1998)**

Texture	Class	% Sand	% Clay
Heavy Clay and Clay	HC/C	23	70
Silty Clay	SiC	10	50
Sandy Clay	SC	55	45
Silty Clay Loam	SiCL	10	34
Sandy Clay Loam	SCL	63	28
Clay Loam	CL	33	34
Silty Loam	SiL	25	15
Loam	L	39	18
Sandy Loam	SL	65	10
Loamy Sand	LS	80	8
Sand	S	93	5

Using the sand and clay contents from Table 2.3 the FC and PWP have been calculated, using equations from Oosterveld and Chang (1980), for surface soils in the given texture classes. These are shown in Figure 2.1 along with available water holding capacity (AWC), defined here as the difference between FC and PWP.

Texture Class	HC/C	SiC	SC	SiCL	SCL	CL	SiL	L	SL	LS	S
FC	39	35	27	30	21	27	23	21	15	12	10
PWP	24	19	16	14	10	13	8	8	5	4	2
AWC	15	16	11	16	11	14	15	13	11	9	7
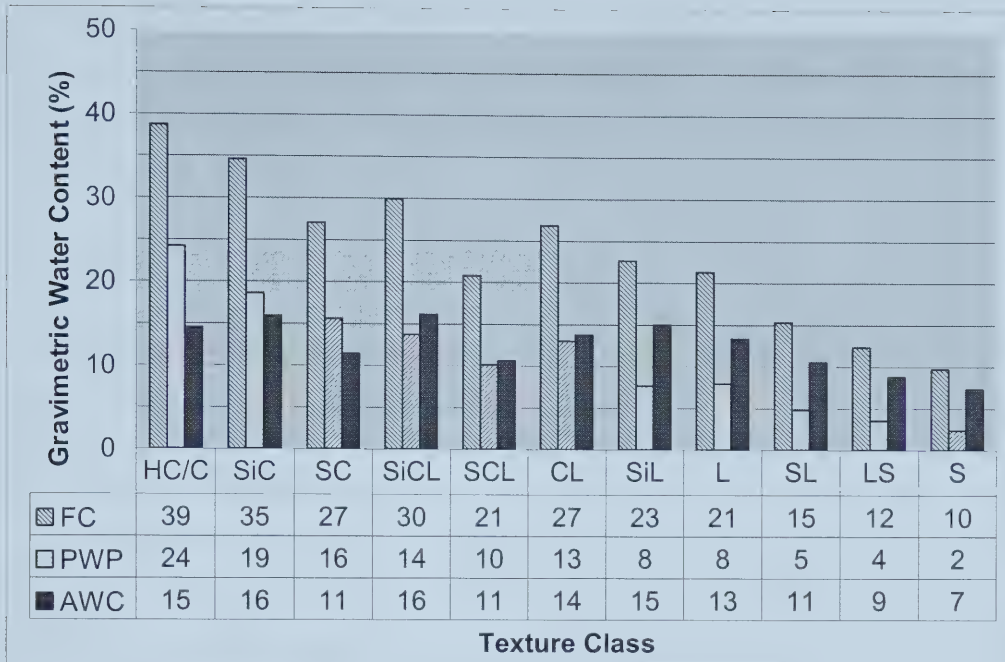
Figure 2.1   Estimated gravimetric water content of selected texture classes (Oosterveld and Chang, 1980)

The importance of converting field estimations of relative available soil moisture to absolute moisture values is underlined in the information presented in Figure 2.1. The AWC of most soils are fairly similar but when the relative available soil moisture is converted to an amount and added to the PWP amount a different picture emerges.   For example, a Sandy Clay Loam (SCL) with 50% plant-available water has roughly the same water content as a Silty Clay Loam (SiCL) with 10% plant-available water. Therefore, both soils may have similar radar image characteristics, all other factors being equal because radar returns are from water molecules rather than derived measures such as plant-available water.

2.1.2   Spatial Data Characteristics

JERS

The SAR sensor onboard the JERS-1 satellite operates in the L-band which has a frequency of 1.275 GHz and a wavelength of 0.235 m. The sensor operates with HH

17

polarization and a nominal incidence angle is 35° (Richards and Jia, 1999). Sensor resolution is 18 x 18 m but the imagery is resampled to 12.5 m pixels with a dynamic range of 16 bits for delivery. More information may be obtained at *http://www.rsi.ca/* (2003, accessed September 2003).

LANDSAT

The Thematic Mapper (TM) sensor on board the Landsat satellite, used here for surface cover characterization, operates in the following bands:

1. 0.45 – 0.52 μm (blue)
2. 0.52 – 0.60 μm (green)
3. 0.63 – 0.69 μm (red)
4. 0.76 – 0.90 μm (near IR)
5. 1.55 – 1.75 μm (mid IR)
6. 10.4 – 12.5 μm (thermal)
7. 2.08 – 2.35 μm (mid IR)

Spatial resolution is 30 m for all bands except Band 6 which is 60 m but resampled to 30 m. All bands have a dynamic range of 8 bits. More information may be obtained at *http://www.rsi.ca/* (2003, accessed September 2003).

Base Features

The Base Features data set, containing the digital base map features for Alberta, are often used for geometric correction of imagery (Dutchak, 2000). The most commonly used feature classes are listed below.

- *Access* – roads and other access features
- *Hydrography* – water bodies

- **ATS** – quarter sections boundaries derived from survey coordinates

- **DEM** – digital elevation model derived photogrammetrically at a grid spacing of 100 m and interpolated to 25 m prior to delivery

2.2 Preprocessing

All spatial data were referenced to the Alberta 10TM NAD83 framework and maintained in a GIS environment. The training site boundaries were delineated on aerial photographs. The photographs were mainly 1:30,000 in scale but ranged from 1: 20,000 to 1: 40,000. The photographs were scanned and each image clipped to the training site area. Each image was then georeferenced using the Base Features data set (Dutchak, 2000) with 4 control points and an affine transformation and then the delineated training site boundary was polygonized using on-screen digitizing. The accuracy of registration was commensurate with the accuracy of the training site boundaries and, in most cases, higher.

2.2.1 Ground Truth

Soil Moisture and Texture

The models developed by Oosterveld and Chang (1980) were used to derive soil moisture content. Texture class was taken from the field survey and converted to percentages of sand and clay using Table 2.3. If more than one texture was present in the soil it was assumed to vary uniformly from top to bottom. At each site FC and PWP were calculated for each centimeter depth of soil[3]. The soil moisture content for each centimeter depth of soil was then derived from the available moisture class noted in the field survey and the definitions in Table 2.2.

---

[3] The field data which are used in this study area were collected for a 90 cm soil depth.

19

The soil profile was divided into depth classes. The criterion for determining depth classes was that there was a significant difference in soil moisture between depth classes for all the training sites. The significance was measured with the Mann-Whitney test at $p = 0.05$. Depth classes were aggregated as required until the differences between depth classes tested significant. The following depth classes were defined.

1. 0 – 10 cm
2. 10 – 30 cm
3. 30 – 50 cm
4. 50 – 90 cm

Surface texture rating was also determined for each site using Table 2.3. Additionally, because two individuals carried out this particular soil moisture survey, the sites were also grouped by surveyor.

Soil Landscape

The application of the expert system (MacMillan *et al.*, 2000) to AGRASID resulted in a soil landform model where each AGRASID polygon was described in terms of the soil(s) most likely to occur in specific slope positions. Determinations were then made as to the dominant parent material and soil genesis at each site. The sites were grouped by soil parent material into "sorted" or "unsorted" indicating deposits of either fluvial/aeolian or morainal origin. The sites were also grouped by genetic disposition as either "Orthic", "Eluviated" or "Solonetzic" indicating either an Orthic Black Chernozem, or a tendency towards eluviation or salinity.

Precipitation

Daily precipitation data representing pre-survey conditions (September 1, 1994 to March 31, 1995) were obtained for stations in the study area (Taggart, 2001). In order to account for missing data in precipitation records an Inverse Distance Weighted (IDW)

interpolated precipitation surface was created for every day of record. IDW interpolation uses a linearly weighted combination of a set of known sample points to estimate the value of any unknown point. The weight is a function of the inverse distance; the larger the weight, the greater the influence of nearby points in comparison to points which are farther away from the unknown point. Shen *et al.* (2000) have shown that an IDW interpolation with a weight of 1 produces the most accurate estimate of daily precipitation given missing data. More information on IDW interpolation can be found in Watson and Philip (1985). The precipitation surface in this study was interpolated to a 10 km grid using the three (3) nearest neighbours and then summed for each day of record. Figure 2.2 shows the over-winter precipitation in the study area prior to the soil moisture survey.
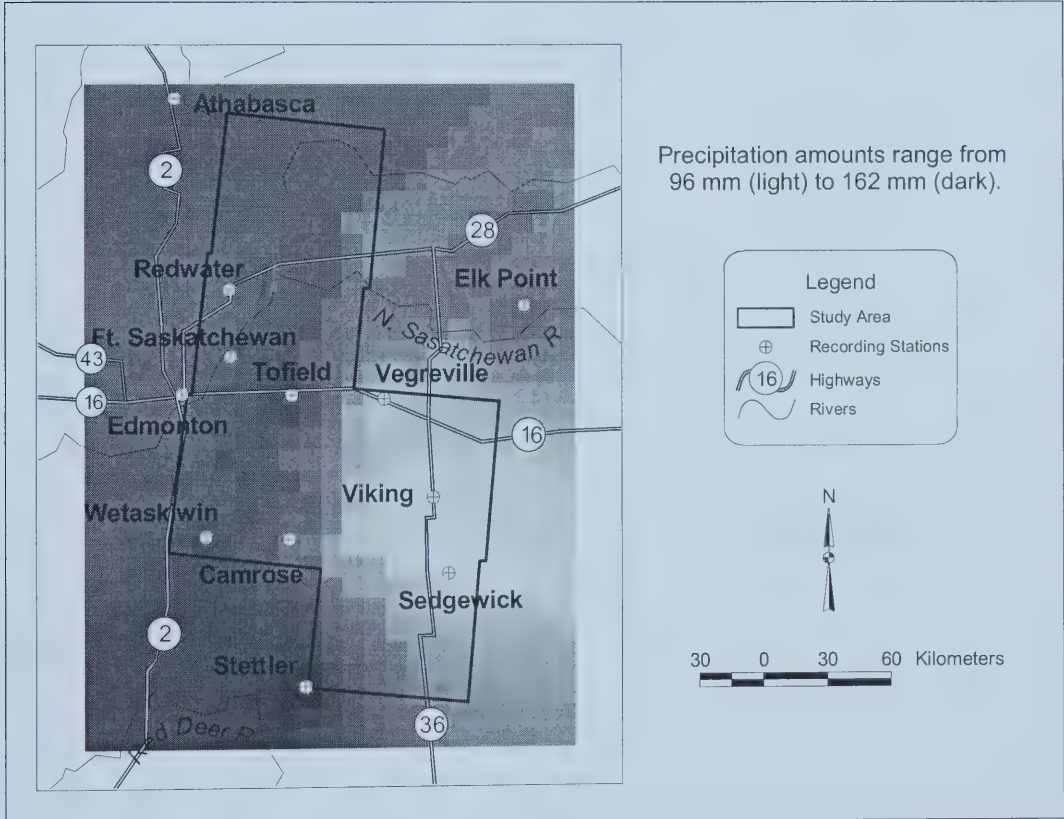
Figure 2.2   September 1994 to March 1995 precipitation

2.2.2 Spatial Data

The imagery acquired is shown in Figure 2.3 and listed in Table 2.4. LANDSAT imagery was used to characterize the amount of crop residue at each training site. Because the study area was covered by imagery acquired on two dates, sites were grouped by image date as "early" or "late". Since a high proportion of sites were imaged by LANDSAT on both days a decision was made to use the LANDSAT image which would more closely correspond to the JERS image date.
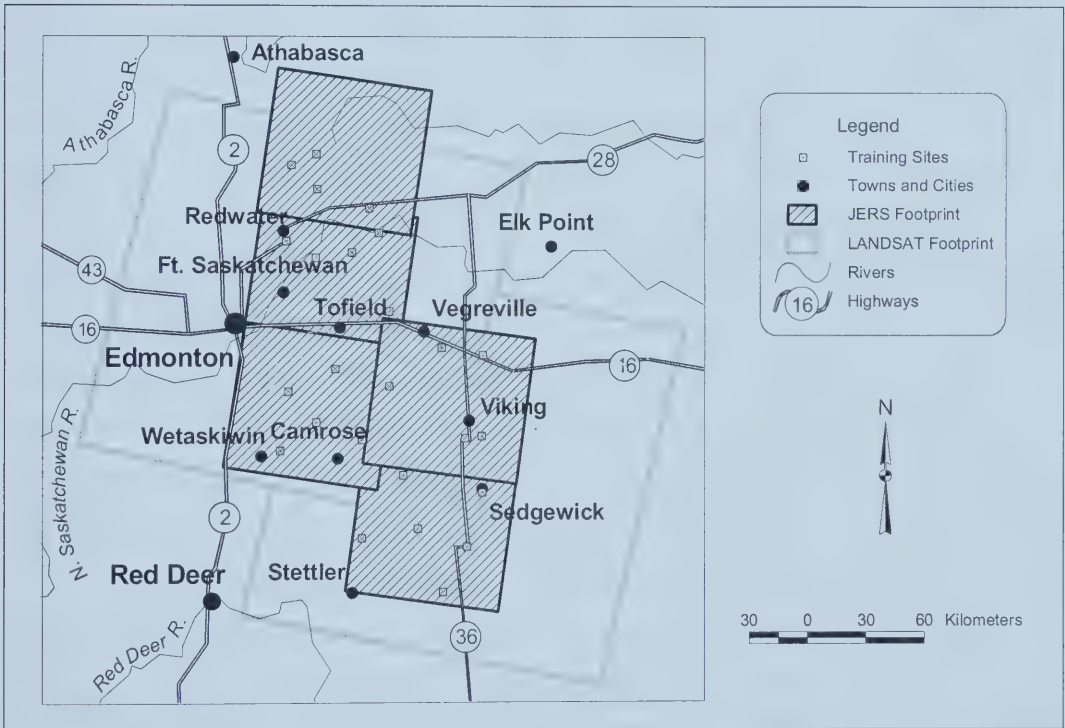
Figure 2.3   Satellite image footprints

Table 2.4   Image acquisition for study

Platform	Path/Row	Image Date	Shift
JERS	538/209	April 13, 1995	
JERS	538/210	April 13, 1995	
JERS	538/211	April 13, 1995	
JERS	536/212	April 11, 1995	
JERS	536/211	April 11, 1995	
LANDSAT	42/23	April 17, 1995	15% south
LANDSAT	41/23	April 10, 1995	35% north

Image Correction

Geometric correction was performed using the Base Features data set (Dutchak, 2000) to locate the training sites on the imagery. The JERS imagery was particularly difficult to correct due to even small relief distortions inherent in imaging radar. Because of this, Guindon and Adair (1992) and others have suggested that the use of a simulated SAR image is critical to the geometric correction of satellite SAR images. Topographic features can then be simultaneously identified on the image and the simulated SAR image and then used as ground control points (GCPs). These procedures have been successfully employed by Cabanayan (1998) with JERS imagery in an area of pronounced relief. However, the relief in the study area is quite·subdued and so it was difficult to identify topographic features. Therefore, the procedure used was to collect 4 GCPs around each training site on the image to ensure that training the sites had a good fit. GCP collection for LANDSAT followed the same pattern. For each image the lowest order polynomial transformation was used to achieve an average root mean square (RMS) error of about half a pixel with a maximum error distance of less than a pixel for any given point. For LANDSAT images this was an affine transformation.

Radar Backscatter

Each JERS image was resampled to 25 m pixels using bilinear interpolation (Lillisand and Kiefer, 2000). This resampling method is a compromise between nearest neighbour and cubic convolution. It alters original pixel values to a lesser extent than cubic convolution and yet provides some smoothing functions to reduce SAR speckle. It also

has the effect of integrating backscatter over a larger area, thus emulating a coarser spatial resolution than the sensor actually provides. No radiometric calibration was performed to obtain actual backscatter values (σ°) because no comparison was made with other microwave sensors and only relative values were required for analysis. However, tests using analysis of variance (ANOVA) were performed to determine the effect of using a 3 by 3 and 5 by 5 median filter on the image.

Simulated SAR

A model has been proposed by Guindon and Adair (1992) for observing the effect of topography on radar returns. A simulated SAR image is generated from a DEM which takes into account the earth's curvature, the altitude of the sensor and the changing incidence angle with range. However, no software was available in this study for implementing the model within a reasonable timeframe. Instead, a hillshade model (ESRI, 1996) was employed in this study. It is computationally much simpler because it assumes a planar surface, a sensor altitude of infinity and a constant incidence angle. The model output is an inverse function of the angle between the illumination vector and the vector perpendicular to the surface and ranges between 0 and 255 with 0 representing areas of low simulated backscatter and 255 representing area of high simulated backscatter.

In this study the hillshade model was employed with an incidence angle of 35° and an illumination azimuth of 101.5°, parameters which was derived from the JERS header files.

Crop Residue

Each LANDSAT image was resampled to 25 m using nearest neighbor interpolation. There was a considerable area of overlap in the two images so a random sample of all pixels as well as a random sample of training site pixels in the overlap area was taken to compare the reflectance between the two imaging dates. A principle components

analysis (PCA) was then performed on each image and the component scores for each band calculated. These scores were converted to standardized z-scores to make both images comparable. Standardized distributions have a mean of 0 and a standard deviation of 1. Since all scores were less than 3 standard deviations from the mean, adding 3 to the score and then dividing the result by 3 achieved a normalized score between 0 and 2. The PCA was performed only on the training site pixels to ensure that they actually did represent crop residue. More information on PCA may be found in Richards and Jia (1999).

Flow Accumulation

A flow accumulation surface was also derived from the DEM to observe the local effects of topography on water accumulation in the landscape and its effect on radar returns. In a flow accumulation model each cell is a measure of the number of cells flowing into it from above. Therefore, the ridges are defined as cells with a value of 0. Depressions must be filled or the algorithm will fail and, therefore, water retention in the landscape may not be modeled adequately. In spite of that, however, the algorithm can provide a unique perspective on the landscape within a training site in terms of the potential amount of water which may infiltrate at, or flow through, any given point. More information on the flow accumulation algorithm may be found in Jenson and Domingue (1988) and Tarboton *et al.* (1991).

In this study the over-winter precipitation grid (Figure 2.2) was used as input to the flow accumulation model to provide a more realistic picture of actual conditions. The output was smoothed by a 5 by 5 mean filter to simulate greater water retention in the landscape.

2.3 Statistical Analysis

Multiple linear regression was used to model the relationship between backscatter and crop residue, simulated SAR and flow accumulation because these parameters could be related on a pixel-by-pixel basis. The error was then compared with soil moisture and

other characteristics, which could only be related on a site-by-site basis, to determine the factor(s) which had the greatest contribution to the residual.

Site-based data (soil moisture) were analyzed by nonparametric methods due to the non-Gaussian nature of the distributions. While nonparametric methods may not be as powerful as their parametric counterparts, they may be more effective in situations where the assumptions of classical methods are not met (Conover, 1971). Spearman's rank-order correlation and the Kruskal-Wallis test of independence between groups were used in this study.

Chapter 3   <u>Results and Discussion</u>

3.1 Image Characteristics

The figures that follow are reproductions of the LANDSAT and JERS imagery. Band 5 was used for the LANDSAT reproductions because it shows the greatest amount of hydrographic detail. The JERS imagery had a 5 by 5 median filter applied to reduce the speckle and then resampled with a pixel size of 25 m using bilinear interpolation. The images are shown without geometric correction applied but each is shown in relative position. Each image has also been contrast-stretched by histogram equalization to visually enhance features.
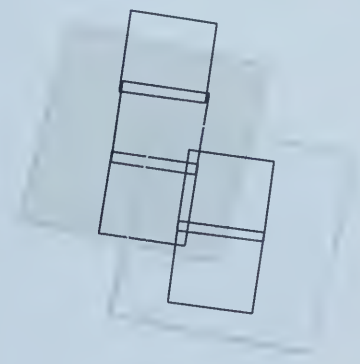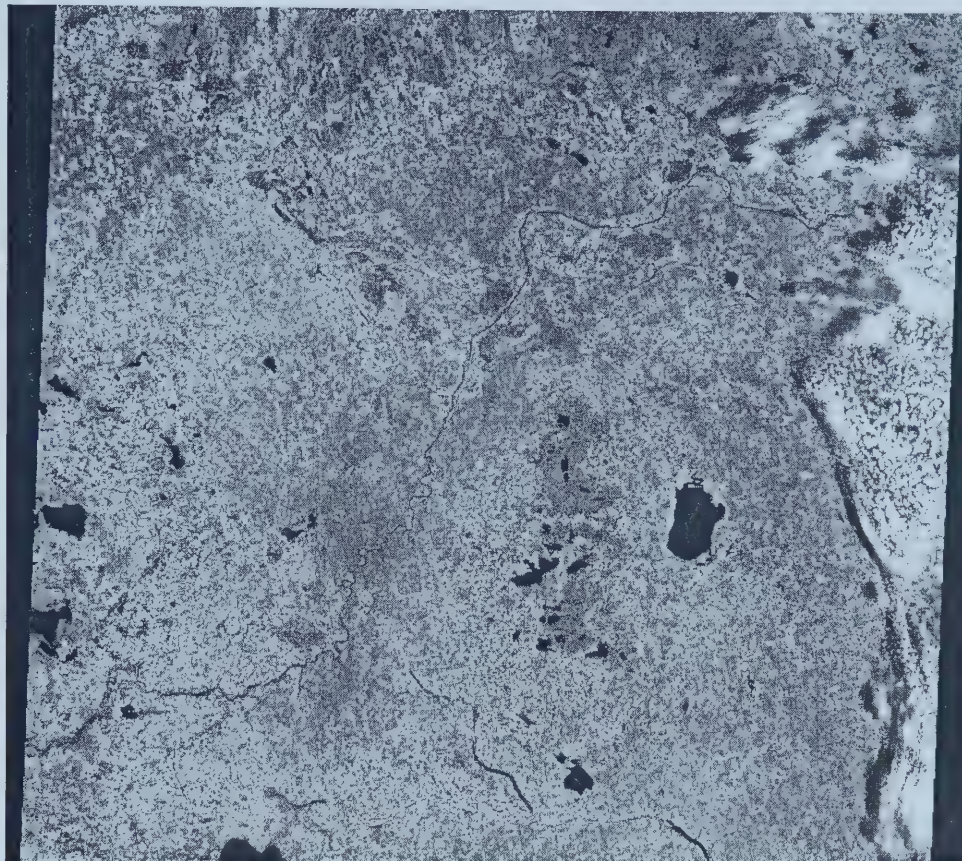
Edmonton, Alberta is approximately in the centre of the image with the North Saskatchewan River running through it from the bottom left (southwest) to the top right (northeast). The water bodies appear black because Band 5 is a water absorption band. Beaverhill Lake is shown prominently to the east of Edmonton and in between is Cooking Lake Moraine. Forested land cover appears darker due to the higher moisture content of the foliage compared with agricultural land cover. The former also has a more mottled texture as opposed to the regular field pattern evident in agricultural areas. The cloud formation with its shadows is distinctive on the right-hand (east) side of the image. Image dimensions are approximately 194 km east-west and 172 km north-south.

Figure 3.1   LANDSAT Band 5 April 17, 1995 (Path 42, Row 23 shifted 35% north)
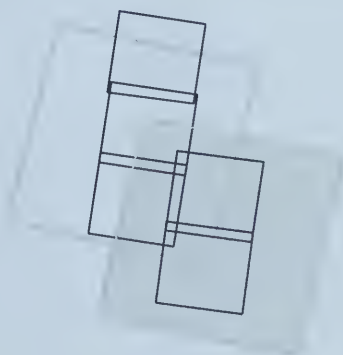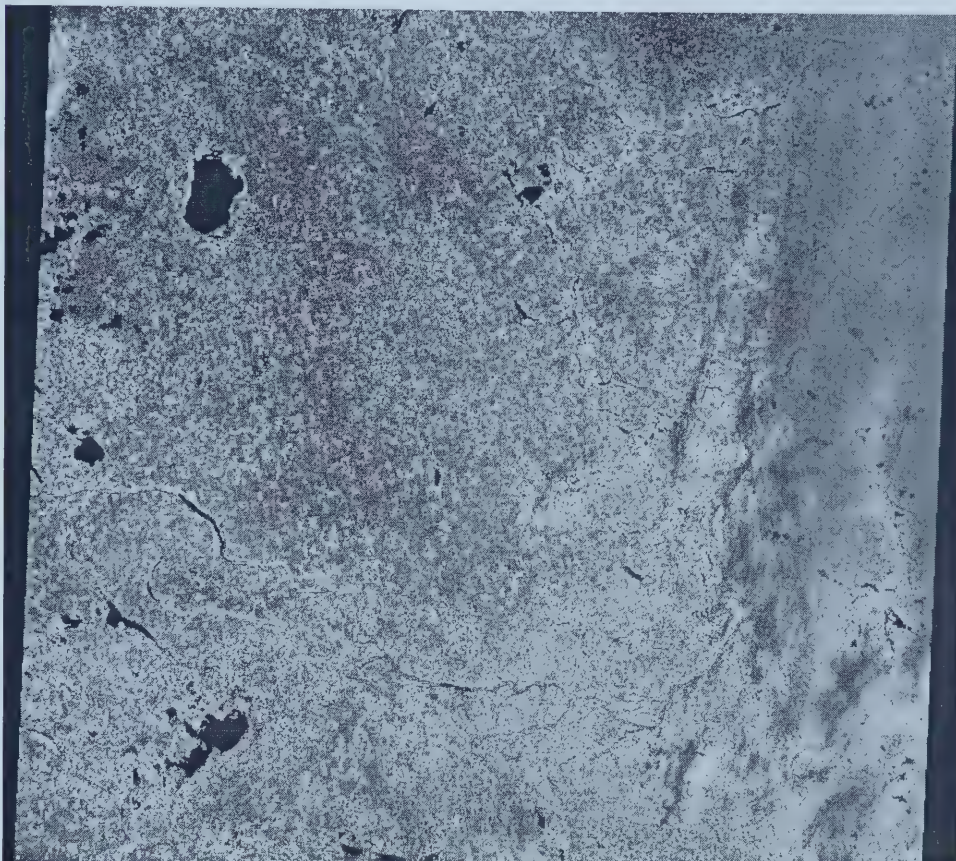
Beaverhill Lake, west of Edmonton, Alberta, is shown prominently in the top left (northwest) corner of the image and the Battle River can be seen to the South, trending towards the east. There appears to be a lighter area in the centre of the image compared with other areas due, perhaps, to drier conditions at that location. The water bodies appear black because Band 5 is a water absorption band. Forested land cover appears darker due to the higher moisture content of the foliage compared with agricultural land cover. The former also has a more mottled texture as opposed to the regular field pattern evident in agricultural areas. A thin cloud formation with its shadows is distinctive on the right-hand side of the image. Image dimensions are approximately 194 km east-west and 172 km north-south.

Figure 3.2   LANDSAT Band 5 April 10, 1995 (Path 41, Row 23 shifted 15% south)
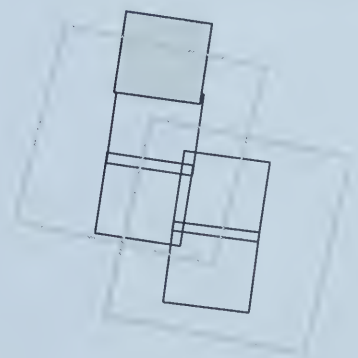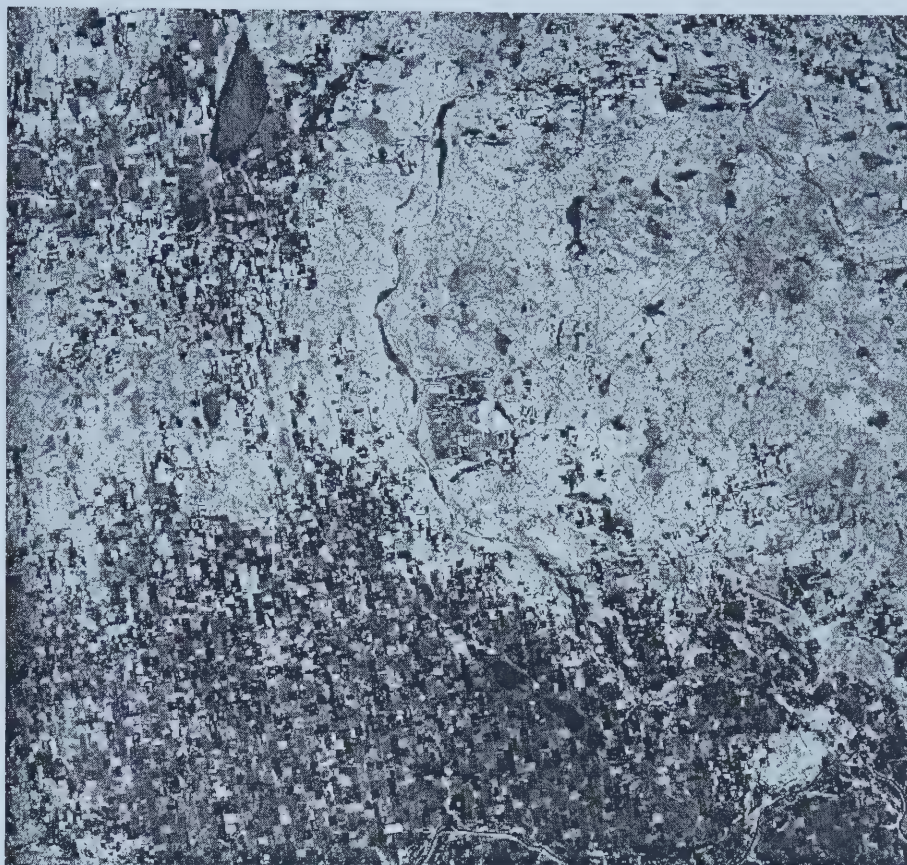
Flat Lake, south of Lac La Biche, Alberta, is shown prominently in the top left (northwest) corner of the image. It has an uneven tone indicating, perhaps, surface water roughness due to wind conditions on the lake. The top (north) part of the image is dominated by forest cover indicating both high moisture conditions and surface roughness. Seismic exploration lines can be seen traversing the area. Image dimensions are approximately 75 km east-west and 80 km north-south.

Figure 3.3   JERS April 13, 1995 (Path 538, Row 209)
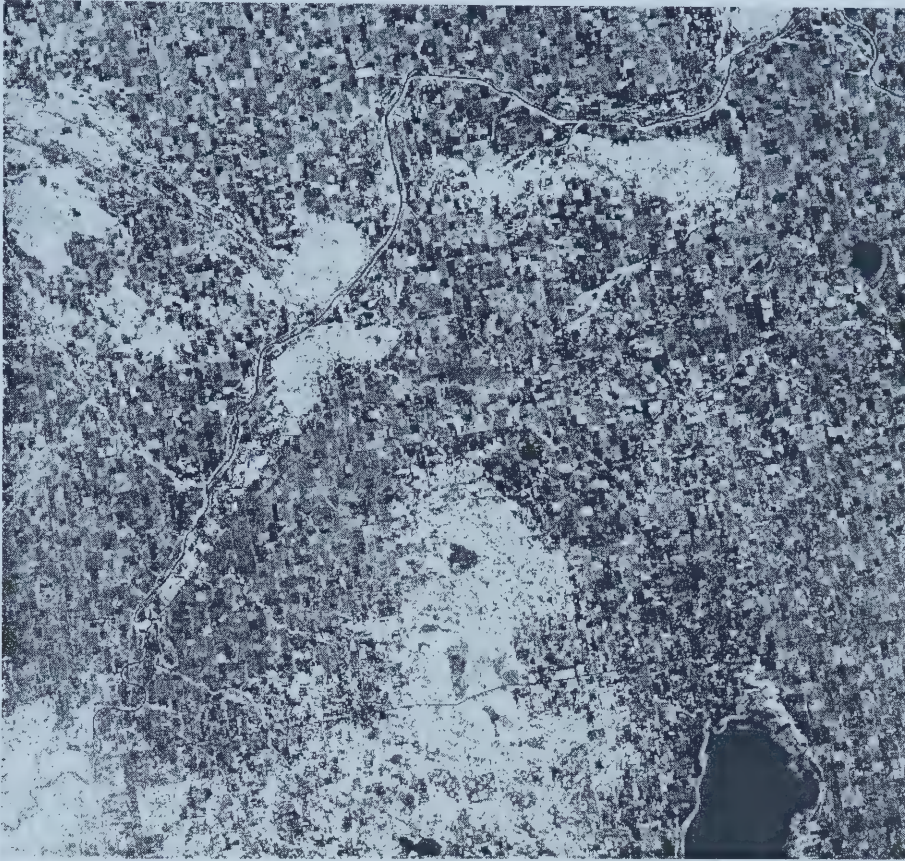
Edmonton, Alberta is shown prominently in the bottom left (southwest) corner of the image. It has a particularly light tone due to corner reflectors in urban areas. Highway 16 extends from Edmonton to the east. The North Saskatchewan River extends from Edmonton to the top right (northeast) corner of the image. The east-facing channel banks have a much lighter image tone because the terrain is facing the sensor and reflecting back most of the signal. Beaverhill Lake can be seen in the lower right (southeast). The light patches interspersed with agricultural land indicate isolated forest stands. Image dimensions are approximately 75 km east-west and 80 km north-south.

Figure 3.4   JERS April 13, 1995 (Path 538, Row 210)
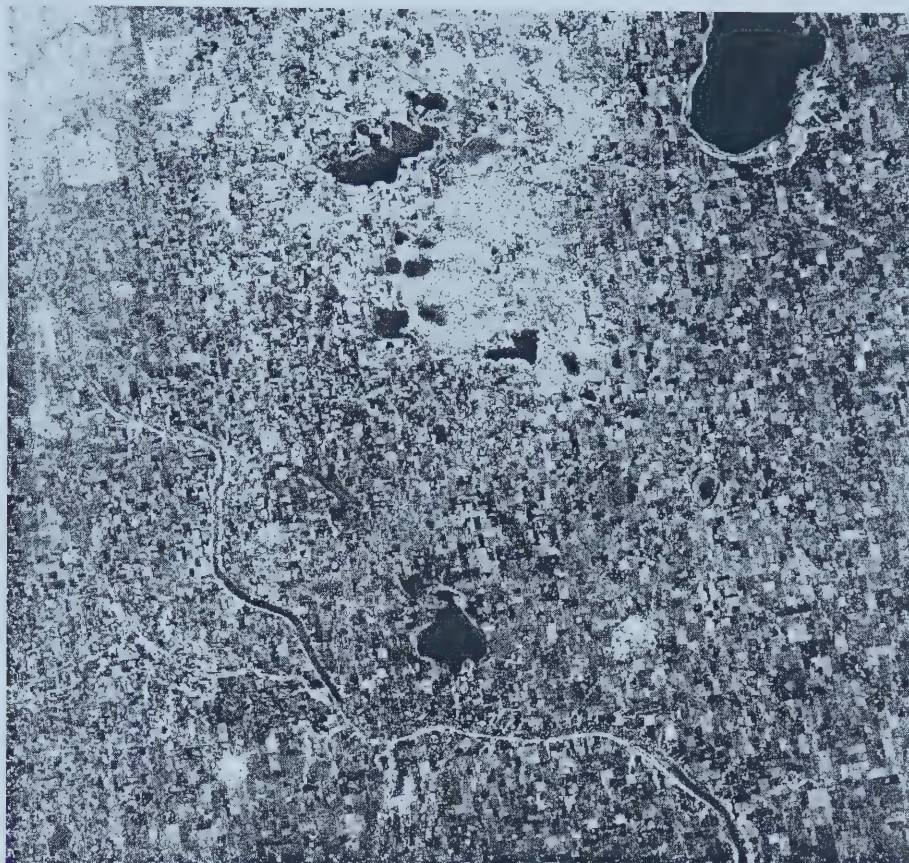
Edmonton, Alberta is shown prominently in the top left (northwest) corner of the image. It has a particularly light tone due to corner reflectors in urban areas. Beaverhill Lake is in the top left (northeast) corner and in between it and Edmonton is Cooking Lake Moraine. The forest cover gives it the light tone due to high moisture and surface roughness. Agricultural field patterns are quite noticeable. Field size seams to increase towards the east. The Battle River system can be seen rising from the left-hand (west) side of the image and trending towards the southeast. Image dimensions are approximately 75 km east-west and 80 km north-south.

Figure 3.5   JERS April 13, 1995 (Path 538, Row 211)
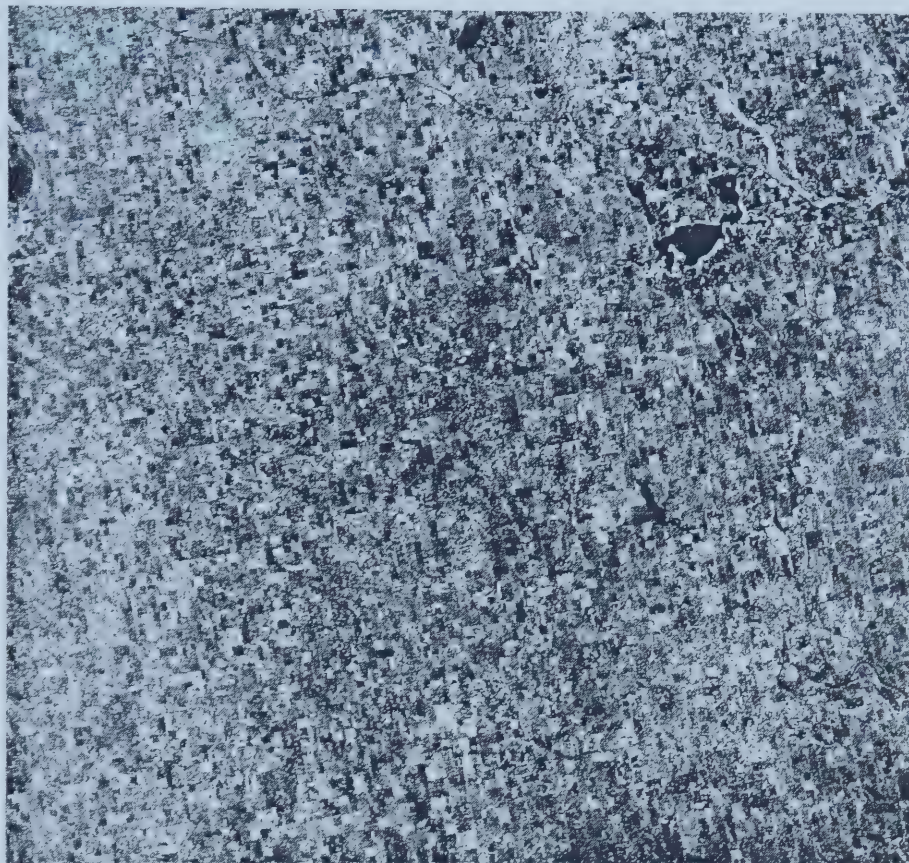
There are not many distinctive features in this image apart from the noticeable agricultural field patterns. A sliver of Beaverhill Lake is showing in the top left (northwest) corner. One other noticeable feature is a generally darker tone in the centre of the image. This may correspond to an area of lower shrub in an area of Solonetzic soil. Image dimensions are approximately 75 km east-west and 80 km north-south.

Figure 3.6   JERS April 11, 1995 (Path 536, Row 211)
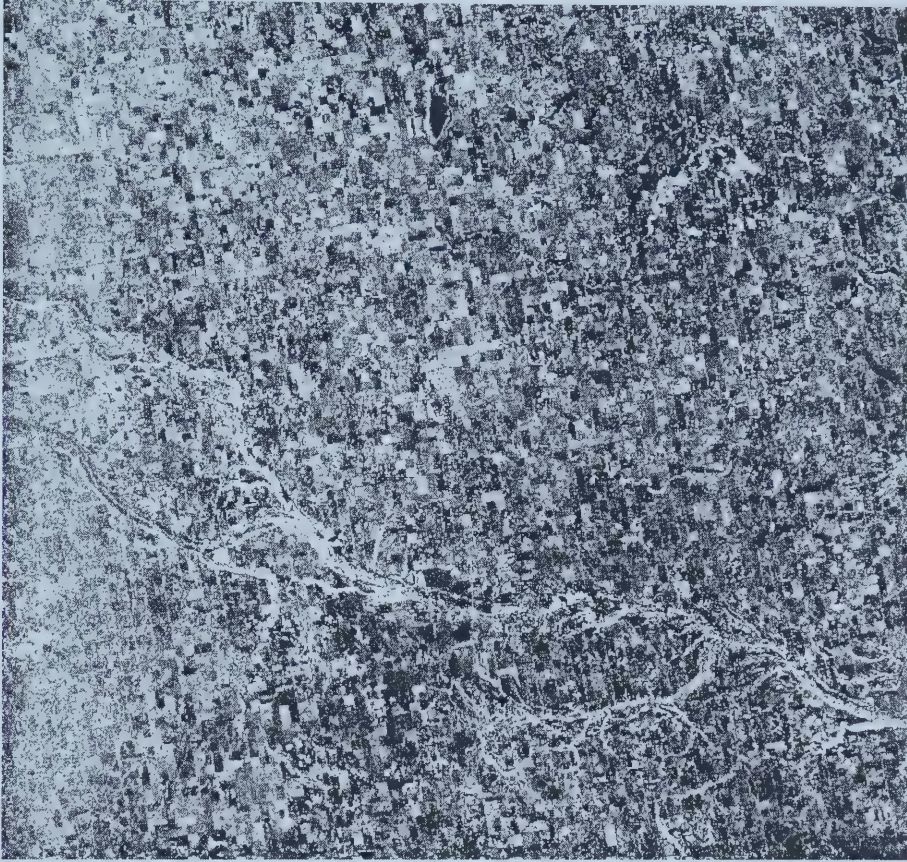
The Battle River system is shown trending southeast from the left (west) side of the image. This is because its valley is heavily dissected and the variable terrain configuration provides a lot of backscatter. The agricultural field patterns are quite noticeable and the general tone appears to decrease from left (west) to right (east). Image dimensions are approximately 75 km east-west and 80 km north-south.

Figure 3.7   JERS April 11, 1995 (Path 536, Row 212)

3.1.1 LANDSAT Multi-date Analysis
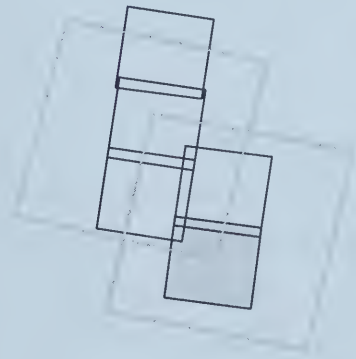
Correlation Analysis

The LANDSAT images for the study area were acquired on two dates seven days apart and had about 40% sidelap. In spring the ground cover conditions can change during that period due to moisture variation and land management practices and these factors may cause a noticeable change in the imagery. Atmospheric conditions may also cause a change in the image characteristics. Six training sites in the study area were located in the sidelap area. Table 3.1 shows the Pearson's correlation of a random sample of pixels in the entire sidelap area and a random sample of pixels in the training sites.

Table 3.1 **LANDSAT image correlation between April 10th and April 17th**

	Entire Sidelap Area (n=5145)	Training Sites in Sidelap Area (n=75)
Band 1	0.83	0.30
Band 2	0.84	0.36
Band 3	0.77	0.39
Band 4	0.59	0.26
Band 5	0.70	0.15
Band 6	0.75	0.86
Band 7	0.66	0.22

In general, the correlation between the image dates in the entire sidelap area is not high with the exception of Bands 1 and 2. These bands detect reflectance in the blue and green parts of the spectrum, areas most sensitive to atmospheric attenuation and which, in early spring, would tend to reflect a change in atmospheric conditions. The high correlation would indicate that atmospheric conditions may have been fairly similar between the two imaging dates. As we move into the longer wavelengths the correlation decreases for several possible reasons: changing moisture conditions, initial plant growth, changing crop residue conditions, and/or commencement of agricultural operations.

The precipitation for Tofield, Alberta, the only recording station in the sidelap area with a complete precipitation record for April, 1995 is shown in Figure 3.8.
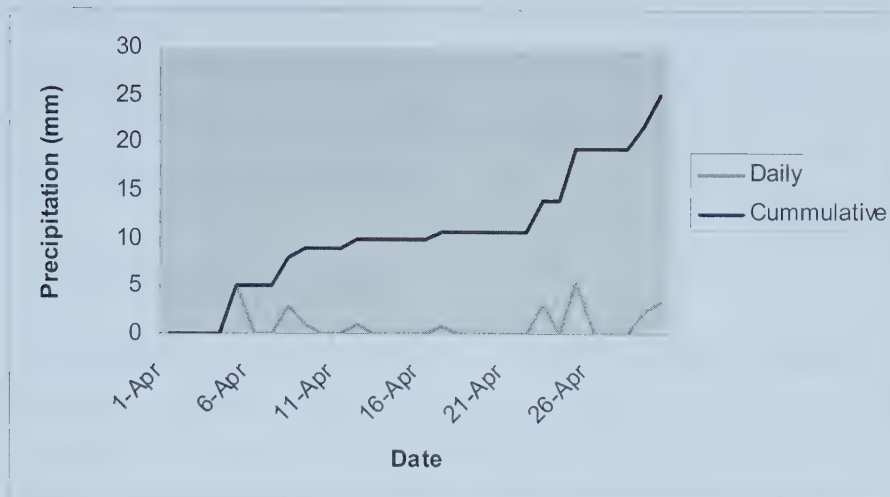
Figure 3.8 April, 1995 precipitation at Tofield, Alberta

Figure 3.8 shows that approximately 3 mm of precipitation occurred between April 10th and April 17th which would add approximately 6 percent of water to the soil volume. However, during that time period, depending on the net radiation and wind, twice as much could be lost to evapotranspiration leaving the soil somewhat drier at the end of that period. The speculated change in moisture status probably would have had the greatest impact on crop residue. This is because crop residue moisture content is much more dynamic than soil and the changes in spectral response *visa vi* changes in moisture status probably much greater.

As far as the training sites are concerned there is very little correlation between the dates in any band with the exception of Band 6. The thermal characteristics of the land surface detected in Band 6 are very similar between the two dates. This may indicate similar air temperatures or may indicate that agricultural operations had not yet commenced by April 17th because once agricultural operations have commenced the thermal characteristics of the land surface can change substantially and would probably be detected in Band 6. However, in spite of this there is still considerable change between imaging dates. This is interesting because all of the training sites are on crop stubble under a continuous cropping land-management strategy. It may be that a precipitation event prior to April 10th, as shown in Figure 3.8, has considerably influenced the image

variability. It may also indicate that the reflectance of agricultural land cover has a greater propensity for change over time, particularly in spring even prior to the commencement of operations, than does general land cover as a whole, probably due to the dynamic nature of crop residue.

Principal Component Analysis

On training sites which have similar crop stubble the primary reflectance material is residue from the crop harvested in the previous fall. As such, most of the reflectance can be inferred as quantity of residue. The results of the PCA to determine crop residue on the training sites on each image are shown in Table 3.2 and Table 3.3.

Table 3.2   Proportion of variance in each principal component in the LANDSAT imagery

	Proportion of Variance	
	April 10th	April 17th
Component 1	0.902	0.888
Component 2	0.067	0.081
Component 3	0.022	0.016
Component 4	0.004	0.009
Component 5	0.003	0.003
Component 6	0.001	0.003
Component 7	< 0.001	< 0.001

Table 3.3   Component loading of each band for the first principal component in the LANDSAT imagery

	Loading	
	April 10th	April 17th
Band 1	0.300	0.203
Band 2	0.194	0.159
Band 3	0.348	0.310
Band 4	0.331	0.337
Band 5	0.696	0.766
Band 6	0.053	0.054
Band 7	0.392	0.366

The analysis provided some interesting information. Firstly, almost all of the variation is assumed by the first principal component, indicating a fairly uniform ground cover because distinctly different cover types would have been manifested in the variation

being spread over more components. Secondly, the difference between the two dates is negligible in terms of component contribution, reinforcing the notion that agricultural operations may have not yet begun by April 17th. The fact that Band 6, which detects thermal emissions, has the lowest loading on either date reinforces that notion as well because, as previously indicated, once agricultural operations have commenced the thermal characteristics of the land surface can change substantially. However, as previously indicated, similar air temperatures on the two imaging dates would also have had an influence.

The component loadings differ between the two dates more than does the proportion of component variance. The highest loading on either date is found in Band 5 and on the later date it is even higher. Since light in the spectral range of Band 5 is absorbed by water, this indicates that surface moisture conditions did change between the two dates. It is unlikely that the change is due to soil moisture depletion to any great extent, particularly in the absence of agricultural operations. It is also unlikely that initial plant growth would make much of a difference in mid-April. However, it could be that crop residue conditions may have changed as a result of evaporation and natural weathering processes. The small amount of precipitation or heavy dew during that period may not have had much impact on the soil moisture status but may have been sufficient to effect the condition of the crop residue. Without specific ground truth it is difficult to be confident of any scenario.

The component loading for Band 1 is lower on the latter date which, contrary to an earlier supposition, may indicate that atmospheric influences on imaging were greater on the later date, particularly when imaging the training sites. In fact, the change in component loading from April 10th to April 17th for Band 1 is opposite to that for Band 5, indicating that, perhaps atmospheric effects did, in fact, play a role in the differences observed in the images. It should be noted that no atmospheric correction was performed so it is impossible to conclude whether the image differences observed at the study sites are a result of atmospheric influences or crop residue conditions, especially considering that no ground truth was collected on crop residue. However, the evidence of a high loading of

the first principal component supports the contention that that particular component reflects the nature of agricultural crop residue in an individual image fairly well but images should be analyzed separately to minimize environmental influences, including atmospheric attenuation. In this study the images have been analyzed separately and the results have been standardized, effectively eliminating image differences due to atmospheric attenuation.

3.1.2   JERS Backscatter

The raw JERS imagery contains a high proportion of noise caused by SAR speckle. Filters are often applied in an effort to reduce the noise and yet retain as much of the data characteristics as possible. To examine the effects of filtering specifically for the sites in this study simple 3 by 3 and 5 by 5 median filters were applied to the entire sample of pixels prior to the application of terrain correction. A visual example of the treatments is shown in Figure 3.9. For display the images have been subjected to a histogram equalization stretch.

| No filter | 3 X 3 Median | 5 X 5 Median |
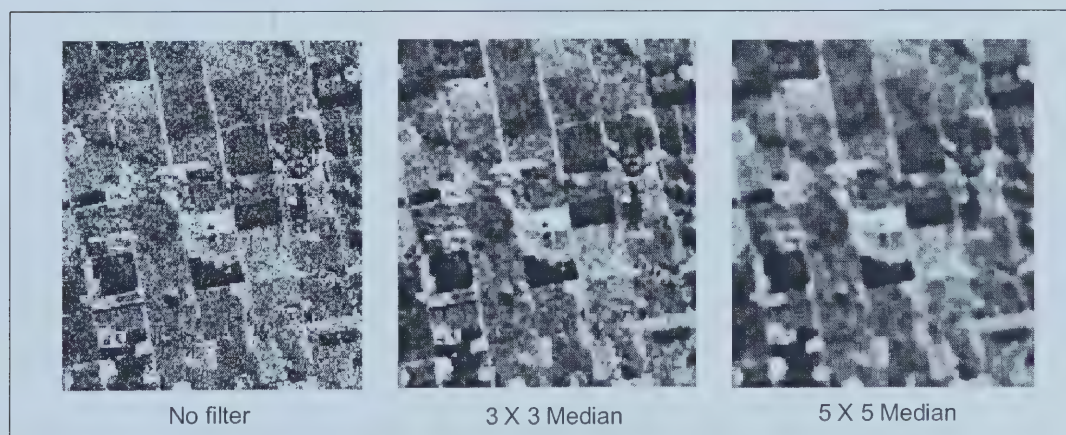
Figure 3.9   Image filtering treatments applied to a JERS sample segment

A visual inspection of Figure 3.9 shows that there is a considerable difference between the filtered and unfiltered images. The 5 by 5 filter looses considerable detail and has the greatest contrast. However, the unfiltered image has considerable noise. The 3 by 3 appears to be a reasonable compromise.

The frequency histograms and selected descriptive statistics for each treatment are shown in Figure 3.10. The distribution of the unfiltered data is definitely different than either of the filtered data sets. The overall range has been reduced by filtering but there is less predictability in the frequency distributions. Generally the frequency has been spread out over the range to a greater extent by filtering, thereby enhancing the contrast. However, the unfiltered data corresponds well to a log-normal distribution and could be easily transformed to reduce skewness and kurtosis.
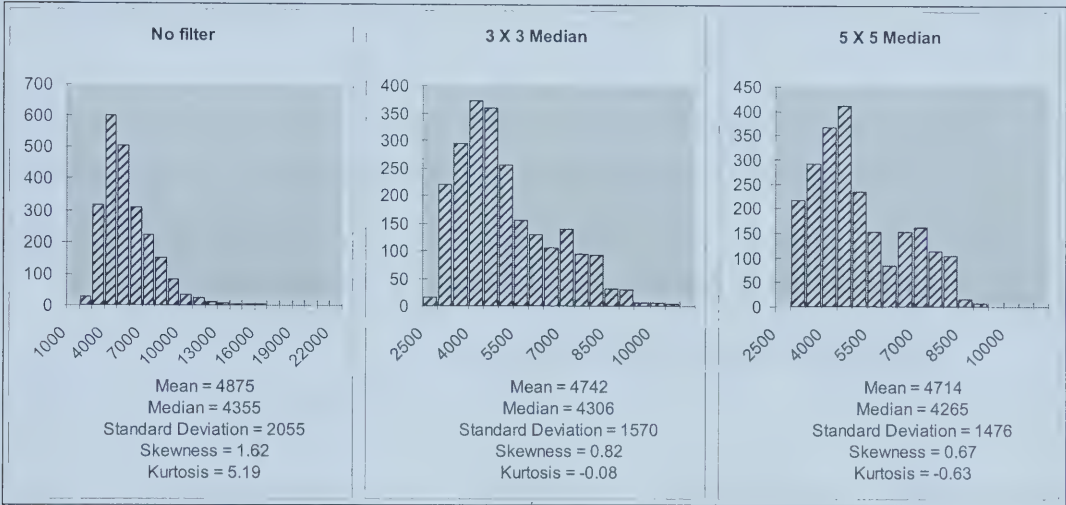
Figure 3.10 Frequency distributions and descriptive statistics at study sites for JERS image filtering treatments

The results of an analysis of variance (ANOVA), including Brown and Forsythe's test for homogeneity of variance, Welch's ANOVA, which is robust to non-Gaussian distributions, as well as the nonparametric Kruskal-Wallis test for independence are given in Table 3.4.

Table 3.4   Analysis of variance (ANOVA) by filtering technique applied to JERS data on study sites

	Value	Significance Level
Classical ANOVA F-statistic	4.52	0.0109
Brown & Forsythe's ANOVA F-statistic	48.8	<0.0001
Welch's ANOVA F-statistic	3.84	0.0215
Kruskal-Wallis χ^2	0.305	0.8585

The tests show that, while the relative differences between the treatment methods are not significant, as implied by the Kruskal-Wallis test, the means and variances are significantly different from each other. However, there is a greater difference in the variances than in the means as illustrated by the Brown and Forsythe test compared with either the classical or Welch's ANOVA. A Duncan Multiple Range test, which tests significance of differences in means based on the standard error of the mean, indicates that the filtering treatments are not significantly different from each other but are distinctly different from the control. The mean and standard deviation of the distributions give the same indication.

The data were also grouped by site to determine the difference that filtering has on interpretability on a site-by-site basis. The results are given in Table 3.5.

Table 3.5 **Analysis of variance (ANOVA) by study site for different filtering techniques on JERS data (all results are significant at probabilities < 0.0001)**

	No filter	3 X 3 Median	5 X 5 Median
Classical ANOVA F-statistic	109.3	451.6	972.1
Brown & Forsythe's ANOVA F-statistic	20.98	37.30	43.40
Welch's ANOVA F-statistic	106.5	507.6	1708
Kruskal-Wallis χ^2	1354	1969	2123

Table 3.5 shows that backscatter is significantly different between sites regardless of the filtering method used. However, the tests also show that differences between the 3 by 3 and the 5 by 5 filtering methods are smaller compared to the differences betwee filtering and no filtering.

The data were also subjected to the Duncan Multiple Range test to determine site separability under different treatments. These results are graphically illustrated in Table 3.6.

Table 3.6   Duncan Multiple Range test classes by study site for different filtering methods for JERS data

No filter		3 X 3 Median		5 X 5 Median	
Site Mean	Classes	Site Mean	Classes	Site Mean	Classes
7558	|	7144	|	7122	|
7358	| |	7030	|	6977	|
6989	|	6679	|	9370	|
6275	|	6208	|	6167	|
6121	|	6111	|	6140	|
5258	|	5186	|	5127	|
5089	|	4947	|	4885	|
5071	|	4839	|	4726	|
4546	|	4452	|	4450	|
4535	|	4405	| |	5503	| |
4486	|	4397	| |	4393	| |
4419	|	4273	| | |	4245	| |
4302	|	4175	| |	4177	| |
4043	| |	4046	| |	4058	|
4036	| |	3915	| |	3891	|
3720	| |	3760	|	3890	|
3624	| | |	3699	| |	3033	|
3611	| | |	3515	| |	3497	|
3575	| | |	3482	| |	3439	| |
3391	| | |	3436	|	3387	| |
3355	| | |	3308	| |	3294	| |
3151	| |	3114	|	3184	| |
3135	| |	3099	|	3130	|
2900	|	2815		2790	| |
2873	|	2807	|	2781	|

These results show that the greatest differentiation in site backscatter is achieved with the 5 by 5 filtering. Most of the sites can be grouped into unique backscatter classes using a 5 by 5 filter in contrast to no filtering where there is considerable class overlap, particularly at the lower end of the range. This is a reflection of the noise inherent in the unfiltered imagery.

Visually, there is difference in the results of each of the filter applications. Imagery which has had no filter applied is considerably noisier than filtered imagery. This can be verified analytically due to the difference in variances. However, filtered data has considerably more contrast and greater site separability but certain visual detail has been

lost. These characteristics increase with the aggressiveness of the filter.

Due to the relative similarities between the filters and the need to retain detail while removing noise, the 3 by 3 median filter was determined to be the most appropriate filtering technique, of those tested, for the particular cover conditions in this study. However, the unfiltered data was retained for analysis and the difference between the filtered and unfiltered image (unfiltered minus filtered) was used to characterize image noise. This distribution is shown in Figure 3.11.

Image Noise

Mean = 116; Median = 0; Mode = 0
Minimum = -6440; Maximum = 14164
Standard Deviation = 1259
Skewness = 1.69; Kurtosis = 12.6
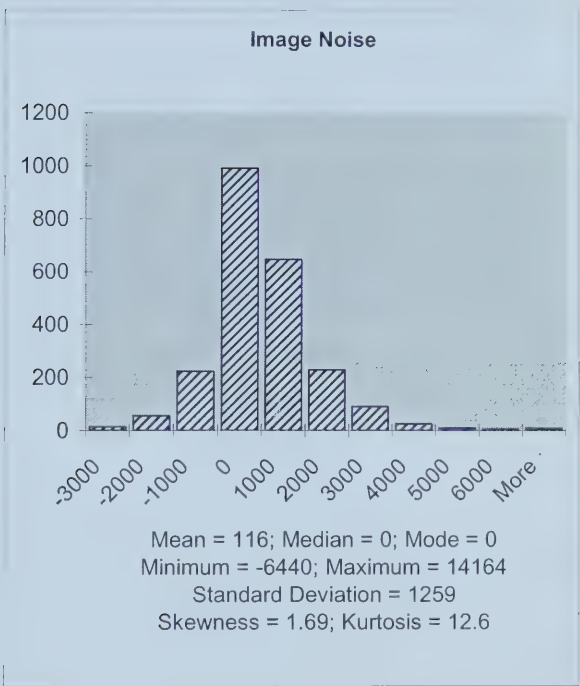
**Figure 3.11 Frequency distribution of JERS
image speckle relative to a
3 by 3 median filter**

The distribution has some interesting features. The median and mode are exactly the same. This implies that there is a considerable number of pixels which do not exhibit any noise and, thus, gives the distribution its marked peakedness. There are a few very dark outliers in the distribution with a few very bright outliers. The outliers tend to balance each other out. Generally speaking, however, most of the noise exhibited in the image is positive (i.e., bright spots in the image). This gives the image its speckled appearance

43

and the distribution its positive skewness. Apart from these unique features, however, the distribution appears fairly normal.

A logarithmic transformation was applied to the JERS image prior to further analysis to achieve a more normal distribution as shown in Figure 3.12.

logarithm of Backscatter

Mean = 3.653
Median = 3.639
Standard Deviation = 0.169
Skewness = 0.23
Kurtosis = -0.01
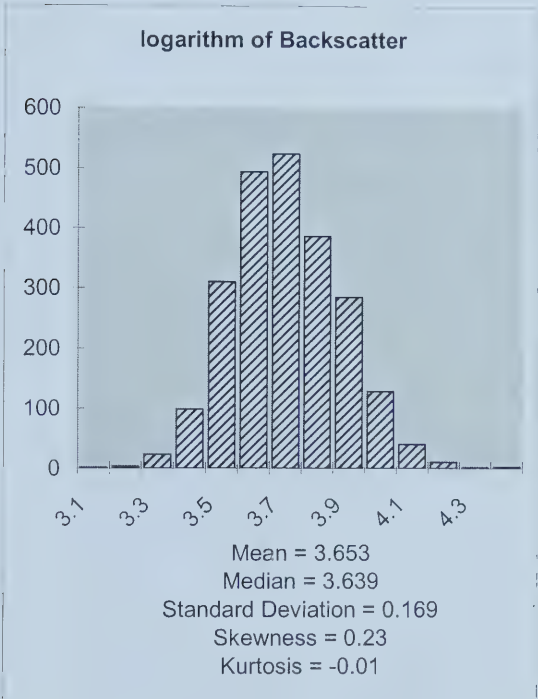
Figure 3.12 Frequency distribution of normalized JERS backscatter

The difference between the raw data distribution and the normalized distribution is immediately noticeable. The shape of the histogram takes on a normal bell-shaped curve, skewness and kurtosis have almost been eliminated, and the mean and median are almost identical. This is reasonable to expect because the actual radiometric calibration equations are logarithmic (NASDA, 1998).

3.2 Surface Cover and Terrain Characteristics

Surface cover and terrain characteristics were obtained from raster data sets. Therefore, the mean was used to characterize tendency and standard deviation used to characterize variability.

3.2.1 Crop Residue

The component scores from the first principal component in the LANDSAT analysis were used as a surrogate for crop residue (see Section 3.1.1). This distribution is shown in Figure 3.13.

Crop Residue

Mean = 1.05
Median = 1.03
Standard Deviation = 0.25
Skewness = 0.03
Kurtosis = -0.07
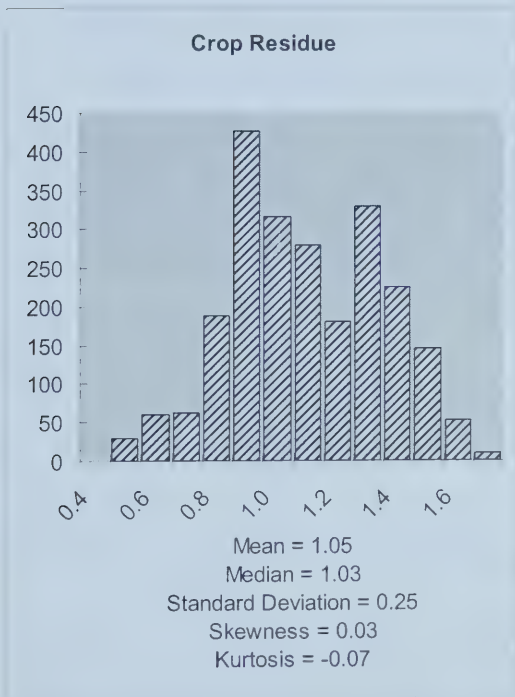
Figure 3.13 Frequency distribution of crop residue scores

Even though fairly uniform land management practices exist throughout the region, there may still be a considerable variation in the reflectance of crop residue as characterized by LANDSAT. Although, statistically speaking, the distribution tends to be normal, there

seems to be two classes. The classes are not distinct and may be separable on the basis of any number of physical factors including type, quantity, quality, etc. Definitely, moisture needs to be considered. Beyond that, however, it is difficult to draw conclusions without firm ground truth.

3.2.2 Simulated SAR

The distribution of the simulated SAR model scores is shown in Figure 3.14.

Simulated SAR

Mean = 145
Median = 146
Standard Deviation = 3.10
Skewness = -1.47
Kurtosis = 5.68
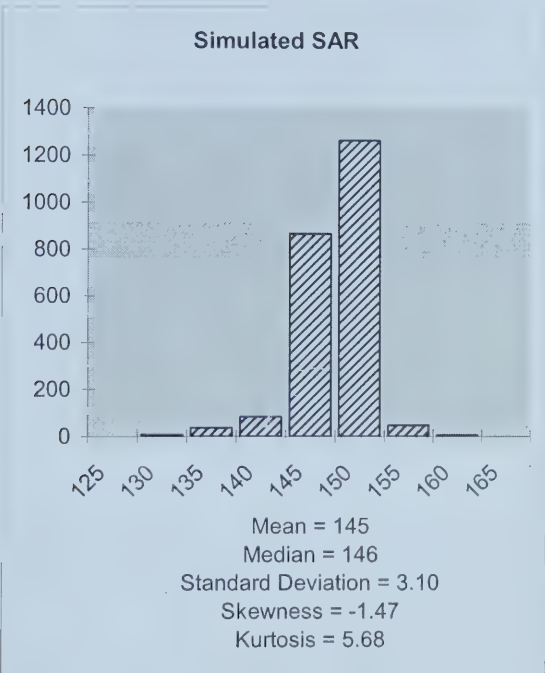
**Figure 3.14 Frequency distribution of
simulated SAR model scores**

One noticeable feature of the histogram is the low dispersion. The shape of the distribution is generally symmetrical (in spite of the high negative skewness) but markedly peaked. This indicates that the variability is fairly low which may be characteristic of a glacial prairie landscape. As a result, the contribution of terrain to radar backscatter variability is likely to be negligible.

3.2.3 Flow Accumulation

The distribution of the flow accumulation model scores is shown in Figure 3.15.
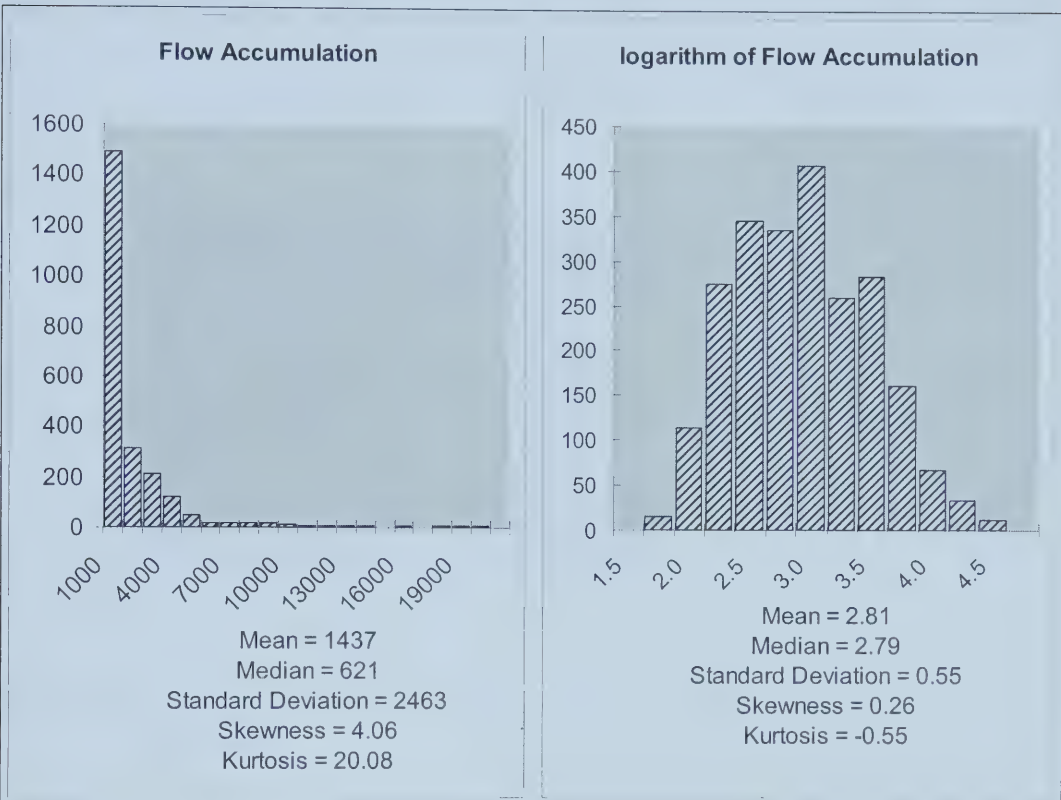
Figure 3.15 Frequency distribution of flow accumulation model scores before and after normalization

The distribution of values produced by the flow accumulation model is a reflection of the fact that only a small proportion of the landscape receives the majority of runoff. The depressions where water does actually collect are small. This indicates that the site variability in terms of water retention in the landscape is fairly low. The logarithmic transformation normalized the distribution quite well and enabled the data to be used in further analysis.

3.3 Soil Moisture and Textural Characteristics

3.3.1 Soil Moisture

Figure 3.16 shows the median and range in each of the four soil depth classes for both absolute as well as plant-available soil moisture.
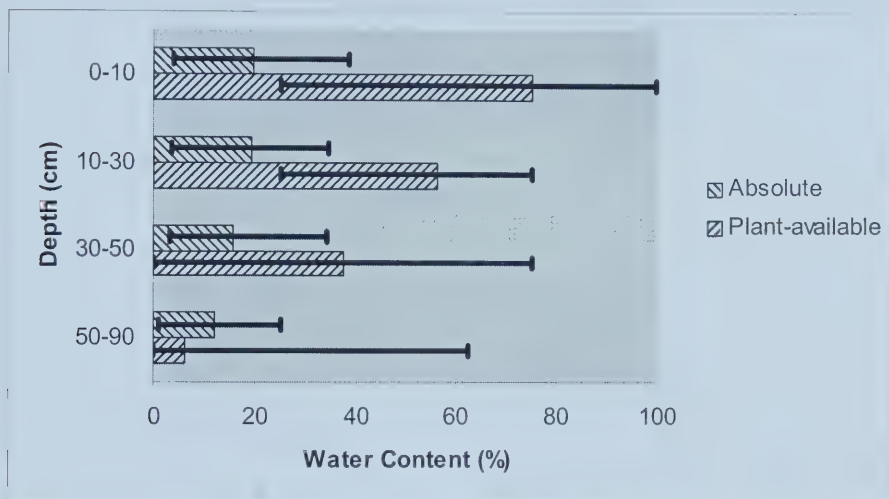
Figure 3.16 Median and range of absolute and plant-available soil moisture

One of the properties of the training sites is the general decrease of available moisture with depth even though the absolute soil moisture varies little. This indicates that the AWC and/or the PWP of soils at these sites may actually increase with depth. This is reasonable to expect if clay content increases with depth (see Table 2.3).

Another interesting property of soil moisture at the training sites is the lack of differentiation in the soil with depth for absolute moisture between sites, both in median values as well as the range and variation. This indicates that the sites have a relatively common hydrologic history. The dispersion about the mean is also low, as shown in Figure 3.17 which is indicative of similar site conditions throughout the study area and, hence, low variability. It may be difficult to draw firm conclusions based on data which

lack variability due to low resolution.
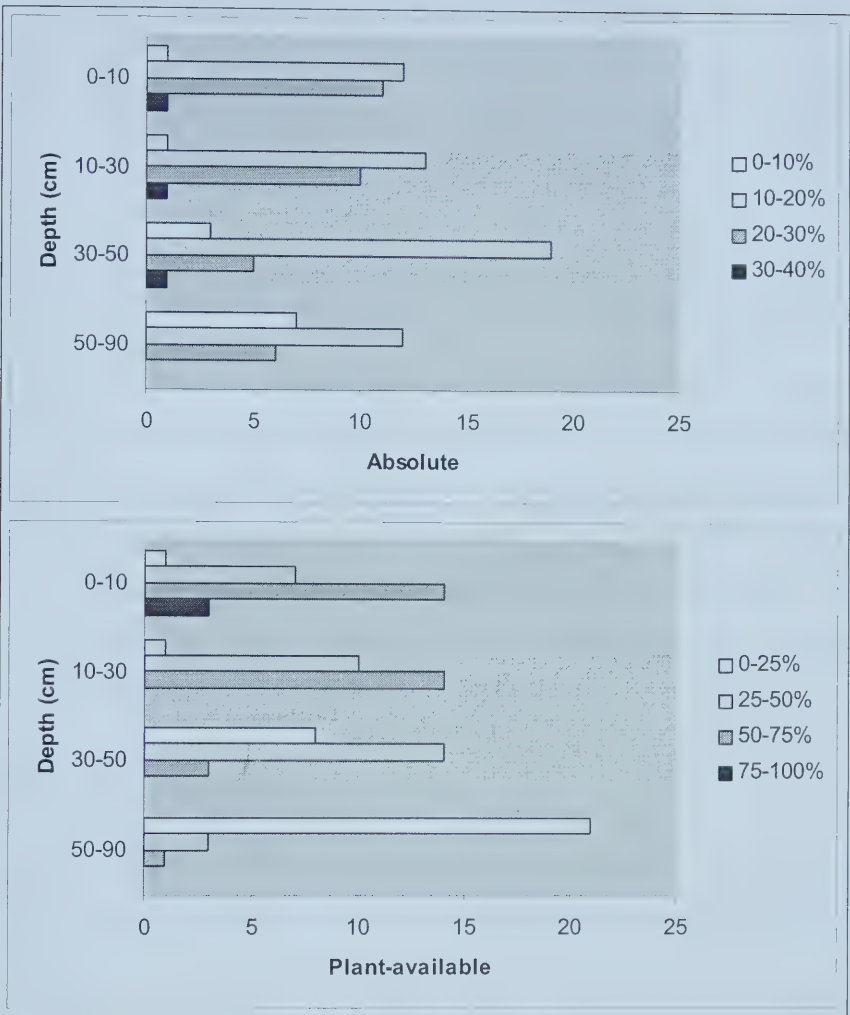
Figure 3.17 Soil moisture frequency distribution

Although depth classes were determined to be significantly different at $p = 0.95$ using the Mann-Whitney test, that test uses the entire sample to measure differences. As seen in the above charts the dispersion of values about the mean as well as the range of values in each depth class is relatively similar between the classes. Figure 3.18 confirms the similarity of soil moisture between depth classes. The lack of differentiation in soil conditions throughout the study area is also demonstrated by the high degree of covariation of soil moisture between depth classes shown in Figure 3.18.
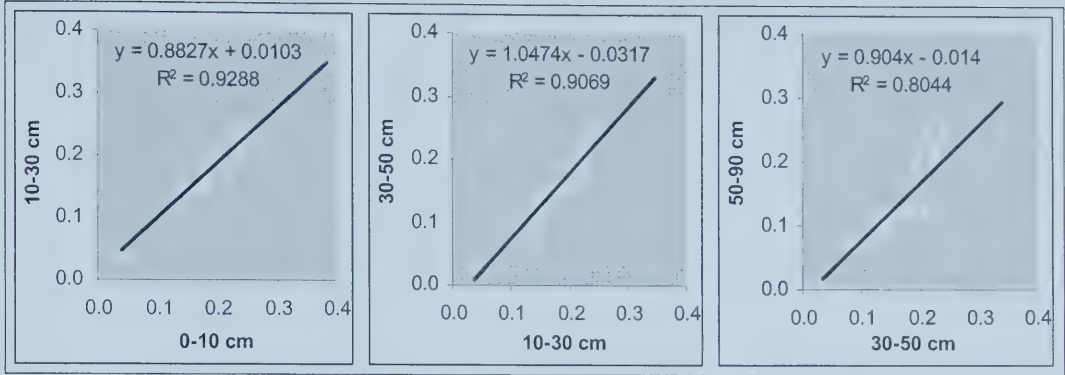
Figure 3.18 Relationship of soil moisture between adjacent depth classes

The high degree of covariation in soil moisture between the depth classes may be indicative of relatively uniform soil characteristics. This calls into question the relevance of sampling below 10 cm. With a few judiciously placed sites where sampling at depth is carried out, a more thorough surface sampling program could be administered to yield highly accurate results from which soil moisture at depth could then be inferred. For this study, due to the high degree of covariation between depth classes, subsequent statistical analysis was restricted to the 0-10 cm depth class.

3.3.2 Soil Texture

Surface soil texture was recorded in the field as a nominal variable. Figure 3.19 shows the statistical distribution in terms of nominal texture classes from higher to lower clay content.
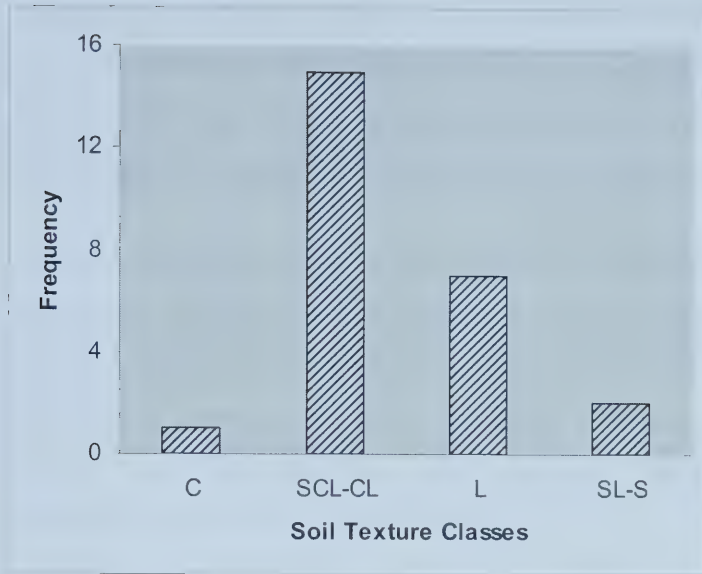
Figure 3.19 Surface soil texture class distribution

The majority of the surface soils are medium textured. This results in moisture retention capabilities which are fairly uniform, demonstrated by the lack of variability in soil moisture throughout the study area. In addition, any potential influence of soil texture in JERS backscatter would also be fairly uniform throughout the study area.

3.3.3 Sampling Bias

There is a question of whether there was a soil sampling bias because two field surveyors carried out the sampling program. Such a bias would be demonstrated by a distinct difference between surveyors in terms of observed soil moisture, particularly relative moisture, and soil texture. Table 3.7 shows the Kruskal-Wallis test for soil moisture and texture by field surveyor.

Table 3.7 Kruskal-Wallis test for soil sampling bias by field surveyor

	χ^2	Probability of Significance
Soil texture	0.8850	0.3486
Absolute Soil Moisture	7.5594	0.0060
Available (Relative) Soil Moisture	1.5706	0.2101

If an actual sampling bias due to individual field surveyors did exist it would exhibit itself in available soil moisture and surface texture, parameters which are observed directly in the field. This is not the case and leads to the conclusion that, in this particular instance at least, a degree of consistency has been maintained throughout the field work.

There is also the question of whether flow accumulation impacts soil moisture. However, Spearman's correlation between mean flow accumulation by site and soil moisture is insignificant ($\rho = 0.0847$; $p = 0.6871$) indicating that most of the over-winter precipitation contributes to runoff. This notion is reinforced by the fact that the Spearman's correlation computed between soil moisture and over-winter precipitation is also insignificant ($\rho = 0.1742$; $p = 0.4050$).

These statistics suggest, perhaps, that either the training areas had moisture in reserve prior to Fall 1994 or that precipitation which fell as snow was blown into ditches or failed to infiltrate the soil at the training sites during spring thaw and, thus, became surface runoff. This observation is important to bear in mind when attempting to model soil moisture dynamics. Winter precipitation may not always be able to function as a surrogate for spring soil moisture, depending on the scale of modeling.

3.4 Interaction of Characteristics with Backscatter

3.4.1 Surface Cover and Terrain

The correspondence between backscatter, crop residue, simulated SAR, flow accumulation and image speckle is shown by the correlation coefficients in Table 3.8. It should be remembered that backscatter and flow accumulation have had logarithmic transformations applied to their distributions.

Table 3.8 Correlation between backscatter, surface cover and terrain parameters (probability of significance is *italicized*)

	JERS Backscatter	Simulated SAR	Flow Accumulation	Crop Residue
Simulated SAR	0.1498 *<0.0001*			
Flow Accumulation	0.2193 *<0.0001*	0.1396 *<0.0001*		
Crop Residue	-0.3431 *<0.0001*	-0.1637 *<0.0001*	-0.2102 *<0.0001*	
Image Speckle	0.5702 *<0.0001*	0.0371 *0.0750*	-0.0034 *0.8692*	-0.0078 *0.7082*

It is interesting to note the high correlation between image speckle and backscatter. This indicates that speckle increases with backscatter due, perhaps, to greater scattering of highly reflective targets. After speckle, the most significant correlation with backscatter is crop residue. Surprisingly, the correlation is negative but the small correlation that exists between flow accumulation and crop residue is also negative. This indicates that crop residue scores may be somewhat related to residue moisture content. Visible light reflectance of crop residue decreases with moisture but backscatter increases. It may also be that the crop residue is lying on the ground surface rather than standing. Thus, it acts as a specular reflector for microwave signals, reducing the backscatter but not affecting reflectance of visible light. However, due to the low correlations and lack of ground truth it is difficult to be definitive with respect to the precise nature of crop residue scores.

The low correlation between simulated SAR and backscatter is also interesting, likely a demonstration of the lack of variability in surface expression of the terrain at the study sites. The low correlation that flow accumulation has with backscatter is a reflection of its relationship with crop residue rather than a reflection of its effect on soil moisture. This is because the correspondence between the flow accumulation model scores and soil moisture and the correspondence between precipitation and soil moisture are both not significant.

A multiple regression analysis was performed to determine the predictive value of crop residue, flow accumulation and simulated SAR for backscatter. The residual error could

then be related to soil moisture and, perhaps, other factors affecting backscatter. Regression coefficients were estimated by entering the variables into the regression in a stepwise manner. Image noise, although, not a physical determinant of backscatter, was included as the final step because of its strong correlation with backscatter. Thus, image noise was not considered when analyzing residual error. The results are tabulated in Table 3.9.

Table 3.9   Multiple regression coefficients for estimating backscatter under various scenarios (probability of significance is _italicized_)

	R^2	Intercept	Crop Residue	Flow Accumulation	Simulated SAR	Image Speckle
A	0.118	3.89	-0.231			
	_<0.0001_	_<0.0001_	_<0.0001_			
B	0.140	3.74	-0.209	0.047		
	_<0.0001_	_<0.0001_	_<0.0001_	_<0.0001_		
C	0.147	3.10	-0.201	0.045	0.004	
	_<0.0001_	_<0.0001_	_<0.0001_	_<0.0001_	_<0.0001_	
D	0.466	3.25	-0.200	0.045	0.003	0.00008
	_<0.0001_	_<0.0001_	_<0.0001_	_<0.0001_	_0.0001_	_<0.0001_

An interesting aspect of these analyses is that, of the variables tested, crop residue has the greatest contribution to the variation in backscatter but adding more variables into the regression model improves the model only slightly. This is probably due to the fact that flow accumulation is somewhat related to crop residue, probably due to the presence of moisture in the crop residue affecting its reflectance, and overall variability of simulated SAR is low to begin with. Although statistically significant there is still a large unexplained variance in backscatter. Much of the unexplained variance can be attributed to image speckle because the R^2 increases dramatically when image speckle is entered into the regression. This indicates that the variation in backscatter seems to be more a function of image speckle than anything else tested here. It reinforces the notion of highly reflective targets causing a relatively high degree of SAR speckle and it also indicates that, in the absence of a strong relationship between backscatter and environmental factors, speckle tends to dominate.

The effect of image speckle may be seen in Figure 3.20 where the results from scenarios

C (excluding speckle) and D (including speckle) from Table 3.9 are graphically depicted.
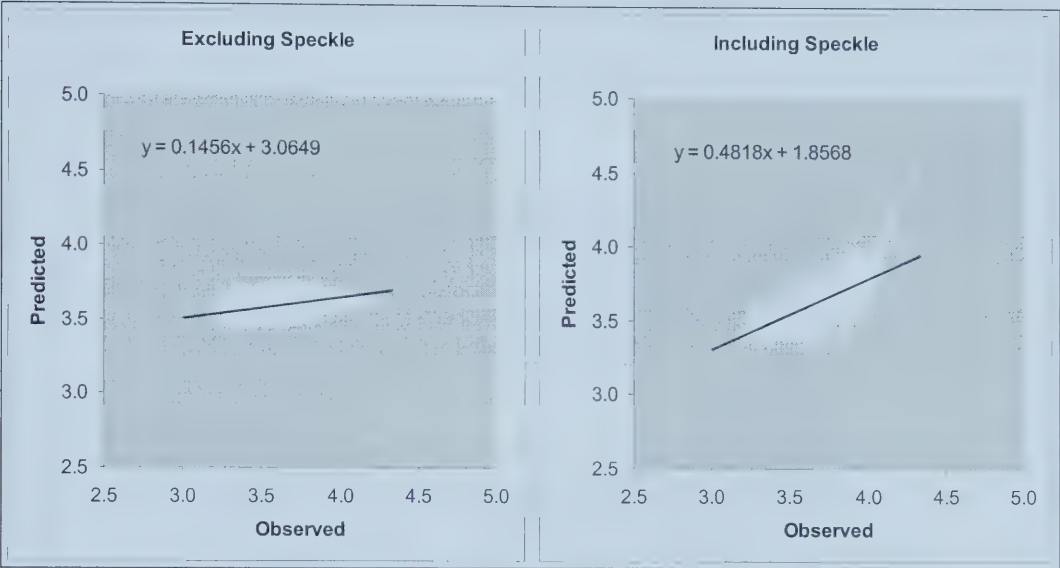
Figure 3.20 JERS backscatter modeled without and with image speckle considered

The scattergram for the model excluding image speckle appears tighter than if image speckle is included in the model. However, because the slope of the regression line is shallow the relationship cannot be considered very strong. The difference in the scattergrams illustrates the effectiveness of image speckle in hiding detail in the imagery which may be useful for interpretation. When speckle is removed subtle features may become apparent. In this case the residual error is not entirely normally distributed and there may be a distinct bias in the error related to some factor other than those in the regression model, particularly as backscatter increases.

3.4.2 Soil Moisture

Regression model residuals were examined to determine possible relationships with other variables. Modeled backscatter was calculated using the best regression model and the calculated values subtracted from the actual values. Using image speckle in the model eliminated that particular effect in the model error term and made interpretation easier. If backscatter is related to soil moisture then there would be a distinct relationship between

the regression model residuals and soil moisture because soil moisture is not considered in the model.

Figure 3.21 shows the scattergram of absolute soil moisture against model residual.
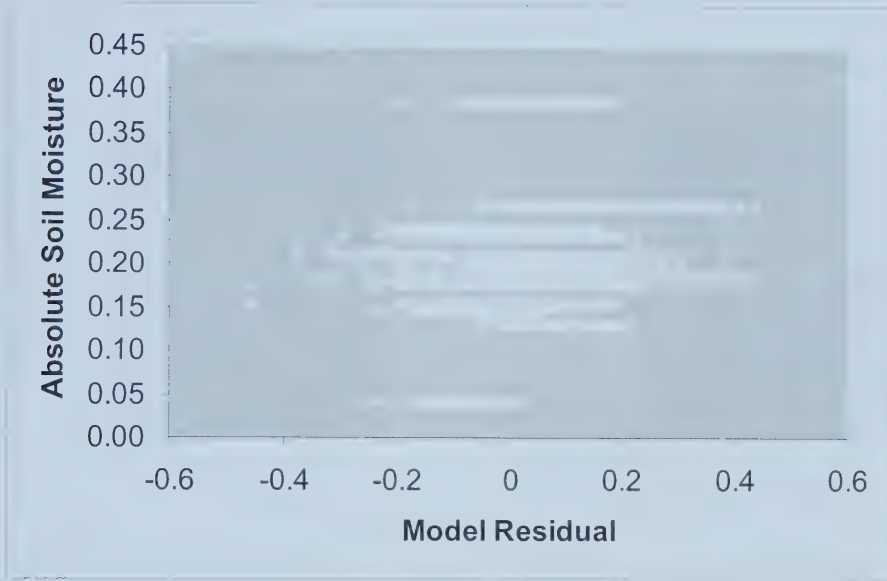
Figure 3.21 Relationship between absolute soil moisture and the regression model residual

The wide scatter of points indicates that there is very little, if any, relationship between the regression model residual and soil moisture. The implication is that, in this type of situation at least, there is very little relationship between backscatter and soil moisture. Even when the low and high soil moisture outliers are ignored in the scattergram, there is very little relationship. This observation is contrary to suggestions in the literature which indicate that soil moisture influences backscatter. However, it may be due to the fact that the exact date of soil sampling is unknown in this study and so the actual soil moisture measurement accuracy may be less than optimal, given the sensitivity of the backscatter regression model. The backscatter from soil may also be confounded by surface residue acting as noise. The residue may have some water in it but it may not be evenly distributed. The sensitivity of the model to image speckle has already been noted and soil moisture measurement accuracy may simply add to the model noise.

3.4.3 Soil Characteristics

Soil characteristics, particularly texture as it influences water holding capacity, can have a considerable influence on backscatter. Figure 3.22 shows the relationship of some soil characteristics to the model residual.
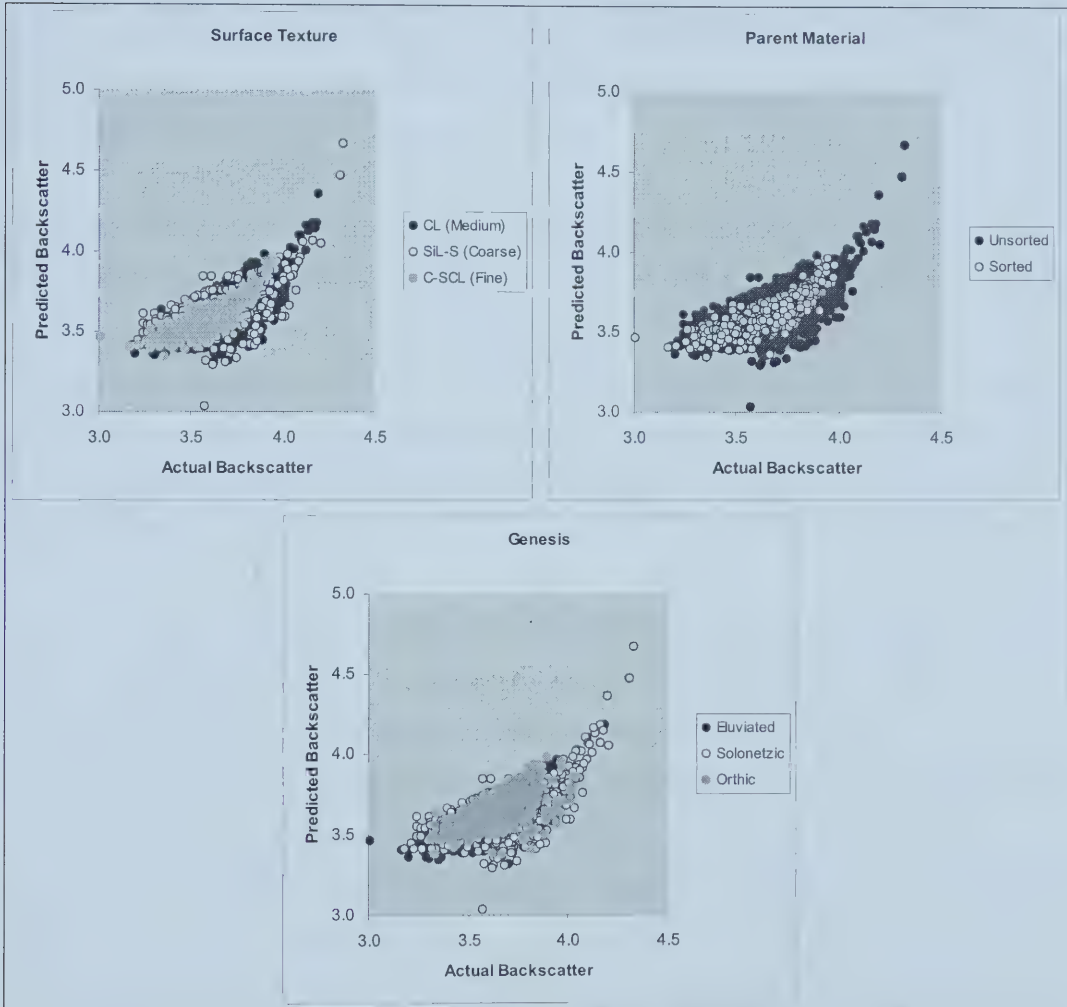
Figure 3.22 Influence of soil characteristics on the accuracy of backscatter modeling

From Figure 3.22 it could generally be concluded that the most reliable estimates of backscatter can be made where soils are fine textured Orthic Black Chernozems on sorted parent material. These are the factors most closely aligned with the regression model. However, without specific ground truth it is difficult to be certain. It may be that these

factors are generally coincident with soils of higher crop productivity and, hence, the sites have greater amounts of crop residue.

3.4.4 JERS Backscatter

Backscatter does not appear to be strongly connected with any of the factors explored here. Even when backscatter within each site is evaluated in relation to crop residue, simulated SAR and flow accumulation, no clear pattern emerges. However, the following observations could be made.

There seems to be some relationship between crop residue model scores and backscatter. Previous studies have shown that backscatter increases with the presence of crop residue so the fact that the correlation between crop residue and backscatter is negative gives strength to the argument that the crop residue model scores may, in fact, not be directly related to the quantity of crop residue but rather to some qualitative aspect. Without reliable ground truth data on crop residue it is impossible to calibrate the crop residue model used here.

There also seems to be a relationship between backscatter and flow accumulation. This could either be due to crop residue or the presence of wet soils. However, flow accumulation has not been shown to correlate with any of the soil and water characteristics examined in this study. Therefore, the relationship is probably due to the presence of moisture in the crop residue which may have a connection with flow accumulation. In addition, when soil moisture levels are low landscape position has little influence on moisture distribution because there is very little free water to move about. From this perspective it could be argued that when conditions are dry crop residue has a much greater influence on backscatter than does soil moisture.

The fact that there has been demonstrated success in relating backscatter to soil moisture under more controlled conditions (Brown *et al.*, 1991; Brisco and Brown, 1992; Geng *et al.*, 1996; and Biftu and Gan, 1999) indicates that with better ground truth, including

water content information, JERS backscatter may also be shown to be related to soil moisture.

Chapter 4   <u>Summary and Conclusions</u>

4.1 Summary

The purpose of this study was to investigate the potential of JERS imagery for detecting soil moisture in an operational monitoring environment. Previous studies have shown great potential for detection of soil moisture with medium wavelength radar imagery, primarily due to its penetration capabilities. Therefore, field soil moisture data were collected from 25 sites in Central Alberta as part of a soil moisture sampling program. The JERS backscatter was compared with soil moisture levels as well as terrain and soil characteristics and surface cover.

LANDSAT imagery was acquired on two dates seven days apart. The difference in the thermal characteristics of the land surface was negligible between the two imaging dates implying that agricultural operations had not yet commenced by the latter date. However, to account for other environmental differences the images were analyzed separately. The PCA revealed that almost all of the variation in reflectance could be found in Band 5. Because all of the sites had crop residue from a similar continuous cropping strategy it was assumed, in the absence of ground truth, that these scores represented reflectance characteristics of crop residue.

JERS imagery was characterized by a fairly high degree of image speckle and it was found that 3 by 3 and 5 by 5 median filtering produced images significantly different than with no treatment at all, particularly in internal variability. It was also found that site differentiation increased with filtering but the difference between the filtering treatments were not as great as the difference between no filter and the 3 by 3 median filter. In addition, much of the visual image detail was lost in the 5 by 5 median filter. Therefore, the 3 by 3 median filter was considered optimal for this situation.

Simulated SAR model scores tended to be fairly uniform across the study area indicating fairly subdued terrain. The flow accumulation model seemed to indicate that most of the

sites were in an upslope position with little internal variability to enhance water collection capabilities. The crop residue scores, however, had a greater range and variability across the study area even though general land management practices were relatively similar throughout the study area.

Soil was generally medium textured and fairly uniform among the sites in the study area. The characteristics of the soil moisture distribution seemed to indicate generally low variability within the soil. It was also found that even though depth classes were determined based on soil moisture differences, the variability between the depth classes was similar. This may have been the result of an inadequate sampling technique or an indication that the soils had generally uniform characteristics throughout their depth. At any rate, further analysis was restricted to the 0-10 cm class.

No bias in soil sampling due to different field surveyors was detected and it was also found that there was very little relationship between flow accumulation and soil moisture.

When relating JERS backscatter to crop residue reflectance, simulated SAR and flow accumulation, it was found that backscatter had a higher correlation with image speckle than with any other variable. This indicates that image speckle increases with backscatter and if there is not a strong and meaningful relationship of backscatter to one or more environmental variables then speckle tends to dominate. The next strongest relationship to backscatter was with crop residue reflectance. However, because the relationship was negative and because crop residue reflectance was also somewhat related to flow accumulation, the crop residue reflectance may have been partially related to moisture content. There was very little relationship of simulated SAR with backscatter, probably due to subdued nature of the prairie landscape.

Surprisingly, when regression model residuals were evaluated, there was no relationship to soil moisture. This may have been due to the fact that precise sampling dates were unknown and that, in itself, would have been a source for considerable error. In addition, the low variability of soil moisture may have also been a problem. There seemed to be a

relationship of model residual to soil characteristics but that may have also been a reflection of soils with greater productivity and, hence, crop residue levels.

In summary, JERS backscatter did not have a strong relationship to any factor explored in this study, least of all to soil moisture. This may have been due to the confounding nature of crop residue reflectance, to the lack of soil moisture variability in the study area or, simply, due to the lack of experimental control (not sufficient ground truth).

4.2 Conclusion

From the evidence provided in this study it would appear that JERS may not be an effective tool for detecting soil moisture, even surface moisture, in an operational monitoring environment, at least for the type of situation in this study. That said, there are several caveats to bear in mind. Firstly, the actual sampling date is unknown except that it was sometime in the month of April. The time difference between sampling date and imaging date may have been enough for environmental conditions to affect the soil moisture status to the point of making any potential correlation meaningless. Secondly, no site data were collected for surface conditions. Surface roughness was not considered. In all likelihood, however, surface roughness was fairly uniform across the study area considering all sites were non-cultivated and under a similar continuous cropping strategy. However, crop residue was considered and yet, only through proxy. Ideally there should have been ground truth for crop residue considering the variability observed, even in spite of relatively uniform general land management practices, particularly because of the inability to distinguish between quantity and quality of crop residue. Thirdly, the variability of soil moisture may have been too small to detect. Had there been sufficient moisture variation within the soil there may have been a clear relationship between soil moisture and the flow accumulation model due to the dominant effect of landscape on soil water accumulation. That may have also shown up in backscatter. Finally, there was considerable image speckle which obscured any potential relationships between soil moisture and image tone. It could be that because of enhanced canopy penetration, L-band microwaves generate greater speckle than, for example, C-band, in

crop residue because of dispersed reflections.

It remains to be seen whether JERS may still be useful for soil moisture monitoring under the right circumstances. In an operational monitoring environment, however, ideal conditions are not always available. Moreover, operational soil moisture monitoring programs are often in place to provide decision-making information, particularly in dry periods.

4.3 Further Research

In spite of the limitations shown in this study, some suggestions are appropriate for improvement of this research. Firstly, the field data collection procedures could be altered to provide greater precision. This would involve precise location of sample sites, at least at their centers, and quantitative measurement of soil moisture. Most importantly, it would involve recording field details including date of sampling and surface cover characteristics. Date of sampling is critical when comparing imaging date with sampling date to adjust for time lag. Ideally, field surveys should be conducted at the time of satellite overpass. Surface cover characteristics are important because they impact backscatter to such a great extent. Secondly, this study could be replicated in another year to see if the results were the same. Another approach would be to replicate the study in more than one area each with differing environments. Previous studies have shown the utility of radar imagery for soil moisture detection and under the right set of circumstances JERS may yet become a useful tool for operational soil moisture monitoring.

References

Biftu, F.G. and T.Y. Gan, 1999, *Retrieving near-surface soil moisture from Radarsat SAR data*, **Water Resources. Research.**, 35:1569-1579.

Boisvert, J.B., Q.H.J. Gwyn, B. Brisco, D. Major and R.J. Brown, 1995, Evaluation of soil moisture estimation techniques and microwave penetration depth for radar applications, **Can. J. Rem Sens.**, 21:110-123.

Boisvert, J.B., T.J. Pultz, R.J. Brown and B. Brisco, 1995, *Potential for synthetic aperture radar for large-scale soil moisture monitoring: a review*, **Can. J. Rem. Sens.**, 22:2-10.

Brisco B. and R.J. Brown, 1992, *Soil moisture measurements with C-band SAR: the CCRS outlook and Oxsome experiments*, **Proc. NHRC Symposium**, No. 9, March 9-10, 135-140.

Brisco, B., R.J. Brown and T.J. Pulz, 1989, *The effects of free canopy water on SAR crop separability*, **Proceedings of IGARSS '89/12th Canadian Symposium on Remote Sensing**, July 10-14, Vancouver, B.C. 424-428.

Brown, R.J., B. Brisco, R. Leconte, D.J. Major, J.A. Fisher, G. Reichert, K.D. Corporal, P.R. Bullock, H. Pokrant and J. Culley, 1993, *Potential applications of RADARSAT data to agriculture and hydrology*, **Can. J. Rem. Sens.**, 19:317-329.

Brown, R.J., R. Leconte, B.G. Brisco, C.A. Hutton, D. Mullins, J.G.Gairns, Q.H.J. Gwyn, R. Protz, J. Fisher, P.J. Howarth, P.M. Treitz, J.B. Boisvert and K.P.B. Thompson, 1991, *Oxford soil moisture experiment (OXOME) overview*, **Proc. 14th Canadian Symposium on Remote Sensing**, May 6-10, Calgary, Alberta, 512-518.

Cabanayan, J.C., Jr., 1998, **Monitoring Forest Activities Using JERS-1 Spaceborne SAR in the Province of Aurora, Philippines: Relationship Between Forest Density and RADAR Backscatter**, M.Sc. Thesis, Department of Renewable Resources, University of Alberta.

CAESA-Soil Inventory Working Group, 1998, **AGRASID: Agricultural Region of Alberta Soil Inventory Database (Version 1.0)**, J.A. Brierly, B.D. Walker, P.E. Smith and W.L. Nikiforuk (eds.), Alberta Agriculture Food and Rural Development.

Crevier, Y., T.J. Pultz, T.I. Lukowski and T. Toutin, 1995, *Temporal analysis of ERS-1 SAR backscatter for hydrogeology applications*, **Can. J. Rem. Sens.**, 22:65-76.

Conover, W.J., 1971, **Practical Nonparametric Statistics**, John Wiley and Sons.

Daughtry, S.T., 2001, *Discriminating crop residues from soil by shortwave infrared reflectance*, **Agron. J.**, 93:125-131.

Dirmeyer, P.A., A.J. Dolman and N. Sato, 1999, *The pilot phase of the Global soil wetness project*, **Bull. Amer. Met. Soc.**, 80:851-878.

Dobson, M.C. and F.T. Ulaby, 1986, *Active microwave soil moisture research*, **IEEE Trans. Geosci. Rem. Sens.**, GE-24(1):23-36.

Dobson, M.C., F.T. Ulaby, M.T. Hallikainen and M.A. El-Rays, 1985, *Microwave dielectric behavior of wet soil – Part II: Dialectric mixing models*, **IEEE Trans. Geosci. Rem. Sens.**, GE-23:35-46.

Dutchak, K., 2000, *Personal communication*, Resource Data Division, **Alberta Sustainable Resource Development**.

ESRI, 1996, **ArcView Spatial Analyst**, User Documentation, Environmental Systems Research Institute.

Elachi, C., L.E. Roth and G.G. Schaber, 1984, *Spaceborne radar subsurface imaging in hyperarid regions*, **IEEE Trans. Geosci. Rem. Sens.**, GE-22:383-388.

Ferraro, R.R., F. Weng, N.C. Grody and A. Basist, 1996, An eight-year (1987-1984) time series of rainfall, clouds, water vapor, snow cover and sea ice derived from SSM/I measurements, **Bull. Amer. Met. Soc.**, 77:891–906.

Gausman, H.W., A.H. Gerbermann, C.L. Wiegand, R.W. Leamer, R.R. Rodriguez and J.R. Noriega, 1975, *Reflectance differences between crop residues and bare soils*, **Proc. Soil Sci. Soc. Am.**, 39:752-755.

Geng, H., Q.H.J. Gwyn, B. Brisco, J. Boisvert and R.J. Brown, 1996, *Mapping of soil moisture from C-band images*, **Can. J. Rem. Sens.**, 22:117-126.

Gillespie, T.J., B. Brisco, R.J. Brown and G.J. Sofko, 1990, *Radar detection of a dew event in wheat*, **Rem. Sens. Env.**, 33:151-156.

Guindon, B. and M. Adair, 1992, Analytical formulation of spaceborne SAR image geocoding and "value-added" product generation procedures using digital elevation data, **Can. J. Rem. Sens.**, 18:2-12.

Hallikainen, M.T., F.T. Ulaby, M.C. Dobson, M.A. El-Rays and L.K. Wu, 1985, *Microwave dielectric behavior of wet soil – Part 1: Empirical models and experimental observations*, **IEEE Trans. Geosci. Rem. Sens.**, 23:24-34.

Homes, M.G., 1990, *Applications of radar in agriculture (Chapter 19)*, **Applications of

Remote Sensing in Agriculture, M.D. Steven and J.A. Clark (eds.), Butterworths, 307-330.

Howard, A., 2000, *Personal communication*, Conservation and Development Branch, **Alberta Agriculture and Rural Development**.

Hudson, B.D., 1992, *The soil survey as a paradigm-based science*, **Soil Sci. Soc. Am. J.**, 56: 836-841.

Jenson S.K. and J.O. Domingue, 1988. *Extracting topographic structure from digital elevation data for geographic information system analysis*, **Photo. Eng. Rem. Sens.**, 54:1593-1600.

Ladson, A.R. and I.D. Moore, 1992, *Soil water prediction on the Konza Prairie by microwave remote sensing and topographic attributes*, **J. Hydrol.**, 138:385-407.

Leblon, B., L. Gallant, F. Bonn and A. Pesant, 1996, *Corn residue assessment from optical and thermal infrared ground-based measurements*, **Can J. Rem. Sens.**, 22:198-207.

Lillisand, T.M. and R.W. Kiefer, 2000, **Remote Sensing and Image Interpretation, 4th Edition**, John Wiley and Sons.

MacMillan, R.A. and W.W. Pettapiece, 2000, **Alberta Landforms: Quantitative morphometric descriptions and classification of typical Alberta Landforms**, Tech. Bull. No. 2000-2E, Research Branch, Agriculture and Agri-Food Canada, Semiarid Prairie Agricultural Research Centre, Swift Current, SK.

MacMillan, R.A., W.W. Pettapiece and J.A. Brierley, 2000, *An expert system for capturing and applying soil survey tacit knowledge to automatically link soils to landform position in soil-landform models*, **Proc. 37th Annual Alberta Soil Sci. Workshop**, Feb 22-24, 2000, Medicine Hat, Alberta, 138-145.

Major, D.J., F.J. Larney and C.W. Lindwall, 1990, *Spectral reflectance characteristsics of wheat residues*, **Proc. Intnl. Geosci. Rem. Sens. Symp. (IGARSS'90)**, 2:603-607.

Major, D.F., F.J. Larney, B. Brisco, C.W. Lindwall and R.J. Brown, 1993, *Tillage effects on radar backscatter in Southern Alberta*, **Can. J. Rem. Sens.**, 19:170-176.

McNairn, H. and R. Protz, 1993, *Mapping corn residue cover on agricultural fields in Oxford County, Ontario, using thematic mapper*, **Can. J. Rem. Sens.**, 19:152-159.

McCairn, H., J.B. Boisvert, D.J.Major, Q.H.J. Gwyn, R.J. Brown and A.M. Smith, 1996, *Identification of agricultural tillage practices from C-band radar backscatter*, **Can. J. Rem. Sens.**, 22:154-162.

McMurtrey, J.E. III, E.W. Chappelle, C.S.T. Daughtry and M.S. Kim, 1993, *Florescence and reflectance of crop residue and soil*, **J. Soil and Water Cons.**, 48:207-213.

NADSA, 1998, *User's guide to NASDA's SAR products*, Earth Observation Research Center, National Space Development Agency of Japan.

Oosterveld, M. and C. Chang, 1980, *Empirical relations between laboratory determinations of soil texture and moisture retention*, **Can. Agric. Eng.**, 22:149-151.

Owe, A., A. Chang and R.E. Golus, 1988, *Estimating surface soil moisture from satellite microwave measurements and a satellite derived vegetation index*, **Rem. Sens. Env.**, 24:331-345.

Pietroniro, A., E.D. Soulis, N. Kouwen and R. Leconte, 1992, *The feasibility of using C-band SAR imagery for basin wide soil moisture mapping*, **Proc. 15th Canadian Symposium on Remote Sensing**, June 1-4, Toronto, ON, 176-180.

Richards, J.A. and Jia, X., 1999, **Remote Sensing Digital Image Analysis**, Springer.

Running, S.W., 1991, *Computer simulation of regional evapotranspiration by integrating landscape biophysical attributes with satellite data*, Chapter 22 in **Land Surface Evaporation: Measurement and Parameterization**, T.J. Schugge and J. André (eds.), Springer-Verlag, 359-369.

Robinson, C., F. El-Baz and V.H. Singhroy, 1999, *Subsurface imaging by RADARSAT: Comparison with Landsat TM data and implications for groundwater in the Selima area, northwestern Sudan*, **Can J. Rem. Sens.**, 25:268-277.

Roth, L.E. and C. Elachi, 1975, *Coherent electromagnetic losses by scattering from volume inhomogeneities*, **IEEE Trans. Antennas and Prop.**, 23:674-675.

Rotunno Filho, O.C.R., E.D. Soulis, N. Kouwen, A. Abdeh-Kolahchi, T.J. Pultz and Y. Crevier, 1996, *Soil moisture in pasture fields using ERS-1 SAR data: preliminary results*, **Can. J. Rem. Sens.**, 22:95-107.

Shen, S.S., P. Dzikowski and G. Li, 2000, **Interpolation of 1961-1997 daily climatic data onto Alberta polygons of Ecodistrict and Soil Landscapes of Canada**, Alberta Agriculture, Food and Rural Development Research Report.

Smith, A.M., M.S. Bullock and C.A. Ivie, 2000, *Estimating wheat residue cover using broad and narrow band visible-infrared reflectance*, **Can J. Rem. Sens.**, 26:241-252.

Smith, A.M. and D.J. Major, 1996, *Radar backscatter and crop residues*, **Can J. Rem. Sens.**, 22:243-247.

Smith, A.M., D.J. Major, C.W. Lindwall and R.J. Brown, 1995, *Multi-temporal, multi-sensor remote sensing for monitoring soil conservation farming*, **Can J. Rem. Sens.**, 21:177-184.

Soil Classification Working Group, 1998, **The Canadian System of Soil Classification**, Agric. And Agric-Food Can. Publ. 1646 (Revised).

Strong, W.L. and J.L. Thompson, 1995, **Ecodistricts of Alberta: A Summary of Biophysical Attributes**, Alberta Environmental Protection, Resource Data Division.

Su, H., M.D. Ransom, E.T. Kanemasu, M.D. Nellis and S. Yang, 1995, *Extracting soil-independent spectral components for estimating oat residue covers*, **Geocarto Intnl.**, 10:61-67.

Taggart, J., 2001, Personal communication, Water Sciences Branch, **Alberta Environment**.

Tarboton D.G., R.L. Bras, I. Rodriguez-Iturbe, 1991, *On the extraction of channel networks from digital elevation data*, **Hydrological Processes**, 5:81-100.

Topp, G.C., S.J. Zegelin and I. White, 1994, *Monitoring soil water content using TDR: an overview of progress*, **Proc. Time Domain Reflectometry in Environmental, Infrustructure and Mining Applications**, September.

Ulaby, F.T., P.P. Batlivala and M.C. Dobson, 1978, *Microwave backscatter dependence on surface roughness*, **IEEE Trans. Geosci. Electronics**, GE-16:286-295.

Watson, D.F. and Philip, G.M., 1985, *A refinement of inverse distance weighted interpolation*, **Geo-Processing**, 2:315-327.

Xu, Q.P., J.B. Boisvert, I. Rubinstein, C. Hersom, R. Protz, and F. Bonn, 1998, *Microwave, visible and near infrared spectral properties as a function of water content in organic soils*, **Can J. Rem. Sens.**, 24:9-16.

Zhuang, X., B.A. Engel, M.F. Baumgardner and P.H. Swain, 1991, Improving classification of crop residues using digital land ownership data and Landsat TM imagery, **Photo. Eng. Rem. Sens.**, 57:1487-1492.